

EFFECTS OF MANUFACTURING INDUCED DEFECTS ON  
MIXED-MODE DELAMINATION KINKING IN COMPOSITE  
LAMINATES

A Thesis

by

YIN AI

Submitted to the Office of Graduate and Professional Studies of  
Texas A&M University  
in partial fulfillment of the requirements for the degree of

MASTER OF SCIENCE

Chair of Committee,  
Committee Members,  
Head of Department,

Remash Talreja  
Junuthula N. Reddy  
Mohammad Naraghi  
Rodney Bowersox

August 2015

Major Subject: Aerospace Engineering

Copyright 2015 Yin Ai

## ABSTRACT

With the superior mechanical performance, such as high strength and stiffness, fiber-reinforced polymer composites are widely used on main structures, like airfoil for aircraft or wind turbine. Manufacturing induced defects draw people's attention for a long time and porosity content was characterized as critical factor that would destroy composite structure. In recent years, it has been noticed that rather than defects' content, the shape, size and distribution are also important.

Some of the research focused on influence of defects on crack propagation along interface. Not much attention has been placed on effects for delamination crack kinking. In the current study, in order to explore how voids affect composites delamination kinking, a double cantilever beam (DCB) model with a delamination pre-crack was simulated under tensile loading condition. By a revised Virtual Crack Closure Technic, the strain energy release rates for crack extension in Mode I and Mode II were evaluated. A parametric research was performed with present of various shapes and sizes of voids in resin area. With applying the mixed-mode fracture criterion, the potential kinking angle was determined. In addition, the effects of circular voids in resin area after delamination kinked out was also examined.

Some of the following results have been found. The delamination in the current DCB model is Mode I dominated fracture process. The failure is governed by dilatational energy and it's an elastic failure problem. Voids located in resin-rich area cause stress perturbation at crack tip and activate the delamination kinking at around 15-degree angle. The parametric study of voids with different geometry shows that elliptical voids compared with circular ones are more threatening to crack branching out. Size of voids is also a critical character that with identical distance from crack tip, larger voids accrete the crack kinking possibility. More importantly, distance between of crack tip and voids, regardless of their size and shape, is the most crucial factor for delamination kinking.

## ACKNOWLEDGMENTS

In the past two years, I received a lot of help and support from many great individuals. I would like to express my gratefulness to my advisor Dr. Ramesh Talreja. With his inspiring teaching method and instruction, I was able to explore interesting topics and get knowledge of frontier for composites research. Thanks to his encouragement, I can finish my thesis successfully. I would like to thank Dr. Terry Creasy Dr. Mohammad Naraghi and Dr. Junuthula N. Reddy for their suggestions and assistance on thesis discussions and writing.

In addition, I would like to thank my colleague Linqi Zhuang. Every discussion and talk with him was meaningful and helpful for study and research. I would like to thank for his help in both study and life. I would also like to thank all my group members for their care and encouragement.

Finally, I would like to thank my parents and Yijun Chen. Their understanding and love is my motivation. I appreciate for their giving and support.

# TABLE OF CONTENTS

	Page
ABSTRACT .....	ii
ACKNOWLEDGMENTS.....	iv
TABLE OF CONTENTS .....	v
LIST OF FIGURES.....	vii
LIST OF TABLES .....	ix
1. INTRODUCTION.....	1
1.1 Statement of interest.....	8
2. NUMERICAL INVESTIGATION ON DCB DELAMINATION	
KINKING WITHOUT MANUFACTURING DEFECTS.....	11
2.1 Characterization of DCB delamination kinking model.....	11
2.2 Finite element model illustration.....	16
2.3 Two-step revised VCCT.....	17
2.4 Mesh refinement and FE validation .....	22
2.5 DCB delamination crack kinking analysis .....	24
2.6 Summary .....	30
3. NUMERICAL INVESTIGATION ON DCB DELAMINATION	
KINKING WITH MANUFACTURING VOIDS IN RESIN-RICH	
LAYER.....	31
3.1 Characterization of manufacturing defects in FE simulation.....	31
3.2 Quantified study of voids on delamination crack kinking .....	34
3.2.1 Effects of circular voids on crack kinking .....	34
3.2.2 Effects of elliptical voids on crack kinking.....	40
3.2.3 Effects of voids with same area on crack kinking.....	43
3.3 Summary .....	45

4. NUMERICAL INVESTIGATION ON MANUFACTURING VOIDS	
IN RESIN-RICH LAYER AFTER CRACK KINKED .....	46
4.1 FE model characterization.....	46
4.2 Effects of circular voids on delamination crack kinking when $t=0.3\text{mm}$ .....	48
4.3 Effects of circular voids on crack propagation within resin layer.....	49
4.4 Stress analysis for crack extension with void.....	50
4.5 Summary .....	56
5. CONCLUSIONS .....	57
REFERENCES .....	58

## LIST OF FIGURES

	Page
Fig 1 Delamination jumps between two interfaces in Mode I DCB test[7].....	4
Fig 2 Damage evolution in general laminate loaded with axial static or cyclic tension[3]	7
Fig 3 Resin-rich area between plies and voids illustration. [11, 12].....	9
Fig 4 Delamination prediction by examining SERR at different kinking angles[13].....	10
Fig 5 DCB delamination model illustration .....	13
Fig 6 Crack kinking illustration in front of delamination crack tip. ....	14
Fig 7 Crack open displacements in x and z direction after crack extends $\Delta a$ .....	20
Fig 8 Two steps crack closure. (a) closing the open in z-direction, (b) closing the open in x-direction .....	20
Fig 9 Finite element illustration around crack tip .....	21
Fig 10 SERR convergence with element size .....	23
Fig 11 Model examine by comparison of J-integral and total SERR.....	24
Fig 12 SERR for Mode I and Mode II when resin thickness $t = 0.1$ mm, no void .....	27
Fig 13 Mode mixity for resin $t=0.1$ mm, no void.....	28
Fig 14 Fracture criterion parameter C with respect to kinking angles when resin $t=0.1$ mm .....	28
Fig 15 SERR for different resin thickness, no void .....	29

Fig 16 Values of fracture criterion with different thickness resin layer.....	29
Fig 17 Illustration of DCB model with void.....	33
Fig 18 FE illustration of voids .....	34
Fig 19 (a) Size of circular voids and $G_I$ (b) Size of circular voids and $G_{II}$ .....	37
Fig 20 Size effect of circular void on crack kinking.....	38
Fig 21 Effect of distance of circular void when $R=30 \mu\text{m}$ on crack kinking.....	39
Fig 22 Mode I SERR increased by elliptical void compared with no void.....	41
Fig 23 Effects on elliptical void on Mode I SERR at different kinked angle .....	42
Fig 24 Size effects of circular void on crack kinking .....	42
Fig 25 The illustration of voids with same area and different shape parameters.....	44
Fig 26 Fracture parameter C for voids of different shapes with respect to kinking angles.....	44
Fig 27 Crack extension illustration .....	48
Fig 28 Effect of circular void on crack kinking when $t= 0.3\text{mm}$ .....	49
Fig 29 Mode separation of kinked crack.....	52
Fig 30 Fracture criterion C for crack extension in resin without void .....	53
Fig 31 Fracture criterion C for crack extension in resin with void .....	54
Fig 32 Integral path illustration at crack tip .....	55
Fig 33 Distribution of Distortion energy density and Dilatational energy density at extended crack tip.....	55

## LIST OF TABLES

	Page
Table 1 Geometric parameter of voids in autoclave composites .....	7
Table 2 Material constants [2].....	15
Table 3 Material constants of homogeneous resin [3] .....	15
Table 4 DCB geometric properties and composite layup .....	15

## 1. INTRODUCTION

In the past 50 years, the use of fiber-reinforced polymer composite materials has seen a steady growth due to the benefits of their outstanding specific mechanical properties, such as high stiffness to weight and high strength to weight ratio compared with traditional structural materials. Composites have large application in aerospace, automotive and wind energy industry[1, 2]. The strict requirements on structural reliability in these area generated wide interest in composite fracture analysis.

In general, a composite fails when it loses its load carrying capability. Considering the different material properties of fiber and matrix and the laminated structure, it is impossible to explain the composite fracture with a single failure mechanism. The failure of fiber composite has been well summarized as a three-step fracture process when loaded with static unidirectional forces or in fatigue loading[3]. For instance, considering a most general case, a multidirectional composite laminate loaded with tensile force along fiber direction is examined. In this loading condition, fracture initiates from the weakest spot of matrix in transverse ply and forms several transverse cracks. With the presence of neighboring plies, matrix cracks are constrained and the number of parallel transverse cracks increases. When applied loads increase, the number of transverse

matrix cracks per unit length will reach its saturation and activates interfacial debond between different oriented plies. Severe debonding separates plies and results in delamination. Further damage occurs with the propagation of delamination and composite fails when cluster of fiber breaks.

Base on literature, delamination occurs before composite's final failure. In fatigue test, delamination occurs at 50%-60% of fatigue life[4]. The formation and propagation of delamination, as a kind of interlaminar damage, destroy the integrity of composite.

During delamination propagation, it separates the well-bonded laminated structure into several independent plies so as to stop the stress transfer between laminates. As a result, delamination accelerates fiber breakage and leads composite to final failure.

Considering the importance of delamination on composite fracture process, much effort has been devoted into identifying the delamination resistance, which is an important value that characterizes delamination property in mode I, mode II or mix-mode condition[5, 6]. Even though the research has been concentrated on identifying exact values of interlaminar crack resistance, it should be noticed that, in many real cases, the path of delamination is not straight and interface crack is able to turn into adjacent plies becoming intralaminar cracks. The curved crack could initiate another delamination

when it reaches a neighboring interface. As illustrated in Fig 1[7], the experiment for mode I delamination extension in double-cantilever beam (DCB) under unidirectional tension shows the curving pattern of delamination within two adjacent interfaces. The crack initiated from the  $90^\circ/90^\circ$  mid-plane but did not propagate along designed interface. It jumped out from the mid-plane into one of the  $90^\circ$  plies until the crack met the  $90^\circ/0^\circ$  interface. With crack open, it propagated in between the upper and lower  $90^\circ/0^\circ$  interfaces. The delamination jumping scenario is also seen in fatigue test for laminated composites. As described in [4], after the first delamination occurs, one of the them in outer plies turns inwards, activating another delamination and breaking fibers when the crack penetrates inner plies. P. Robinson and D. Q. Song noticed the crack branching and kinking problem in a DCB delamination resistance test[8]. The crack curving between two adjacent plies is commonly regarded as the cause for increase of delamination resistance, addressed by Chai [9].

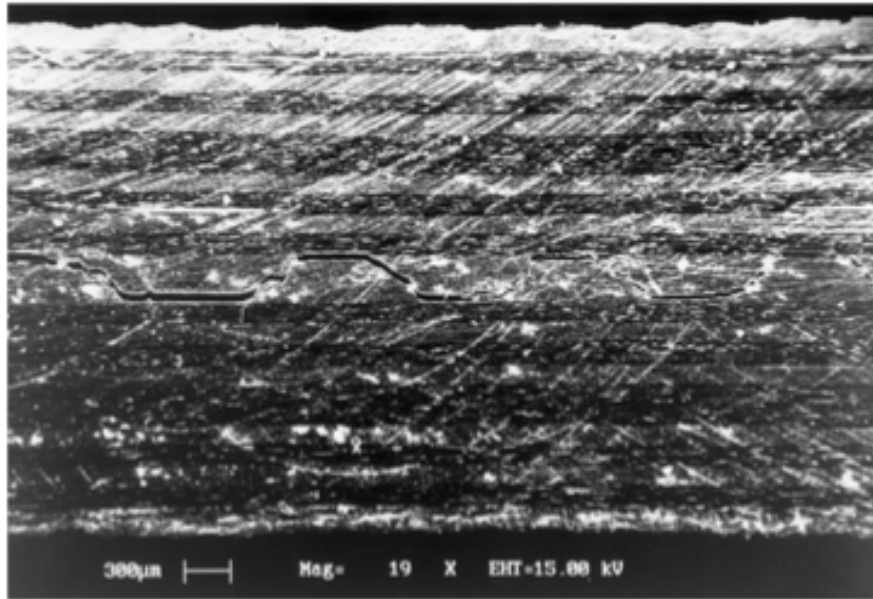


Fig 1 Delamination jumps between two interfaces in Mode I DCB test[7].

Limited by the cost of industrial manufacture, defects generated during composite fabrication are widely distributed, which includes fiber breakage, resin unevenly distributed, voids, etc. Among these, voids are most common defects. Many researches have been performed to explore influences of voids on composite mechanical properties. As a kind of matrix flaw, the material properties dominated by matrix, such as interlaminar shear resistance (ILSS) have drawn people's attention. The extensive studies on relation between ILSS and voids show that the decrease of ILSS is linearly related with void content in end north flexure test for unidirectional composites[10]. Some of the research concluded that with the void contents between 1% to 4%, composite mechanical performance would not be affected [8].

Even though void content, which is easily gained from observation, has been widely explored, some of the current experiments show that it is not sufficient to explain the influence of voids on composite fracture. In the investigation of void effect for static flexural failures, the explorers found the voids played a major role in crack extension as the large voids located in these resin rich regions joined together forming a crack[11]. More and more researchers have realized the importance of voids of different shape, size and distribution on material mechanical properties[9, 12]. Zhu Hong-yan found void induced crack initiation and propagation in interlaminar shear strength test [9]. In addition, M. Ricotta and R. Talreja performed research on Mode I delamination growth with voids in the path of delamination crack[13]. It has been noticed that when the crack approaches defects, the stress perturbation around the crack tip is large and stress energy release rate are over 2 times of the case without voids. From increasing number of research, we can see that the details such as shape, size and distribution of voids are more critical on composite fracture initiation and propagation. It is important to investigate voids through a quantitative analysis on delamination kinking.

Voids' shape, size and distribution are extremely depending on manufacturing process. Autoclave and liquid composite molding (LCM) which includes resin transfer molding

(RTM) are two major composite fabrication technologies. The morphology and distribution of voids produced in the two processes are different.

In autoclave, the prepregs (pre-impregnated fibers) are stacked together on mold to form the composites. During prepreg layup, air could be trapped between plies. In composites curing process, when the composite is squeezed by vacuum or applied pressure, most of the trapped air will be driven out of the structure. The air left over becomes voids in structure. Most of voids in autoclave are constrained within resin-rich area and they are flattened into cigar shape. In LCM process, composite mold is filled with dry fiber matting or fabric. Liquid resin will be pumped in and penetrate fibers. Air flows together with resin but not all of them can be carried out. The left air becomes voids in composite. Voids in produced in LCM have many different shapes and sizes and they can locate near and within fiber tows. The manufacturing-induced voids in autoclave process has been well summarized by Huang and Talreja[12]. In autoclave, both circular and cigar shape voids has been observed. The geometric distribution of voids is listed in Table 1.

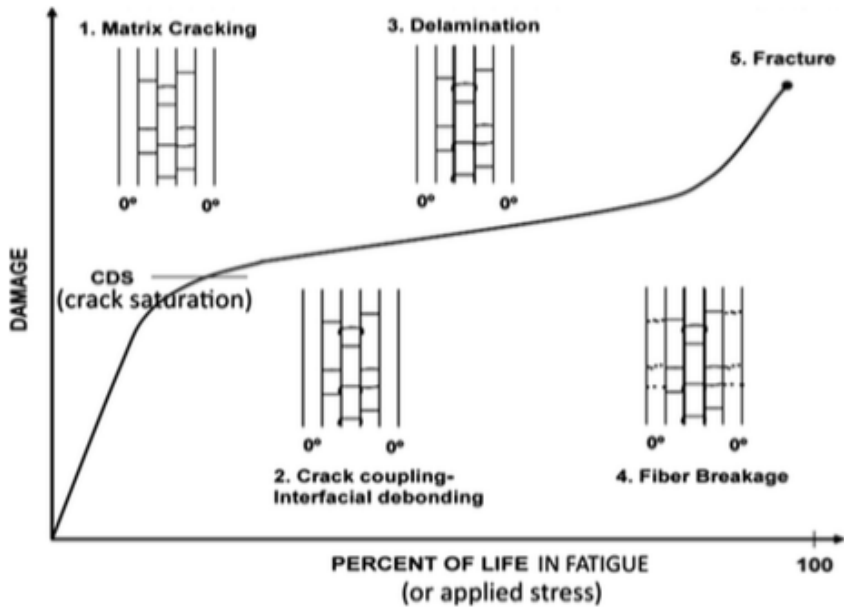


Fig 2 Damage evolution in general laminate loaded with axial static or cyclic tension[3]

Table 1 Geometric parameter of voids in autoclave composites

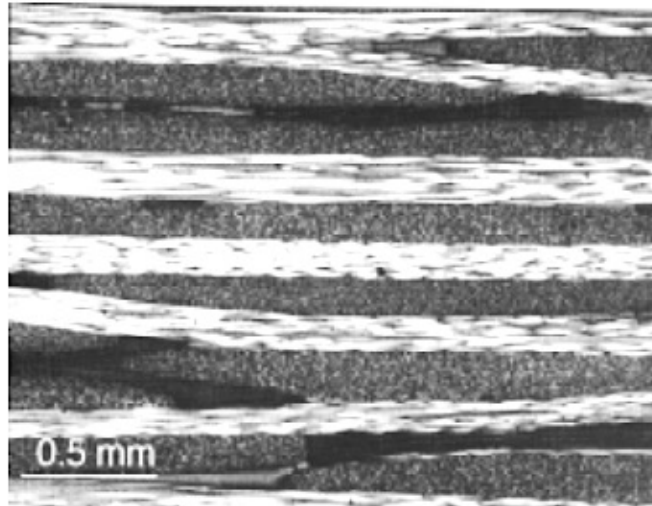
	Length	Width	Height
Range	0.1 to several mm	10 $\mu\text{m}$ to 1mm	5-100 $\mu\text{m}$
Average	0.3 to 1 mm	30 to 100 $\mu\text{m}$	8 to 20 $\mu\text{m}$

Manufacturing-induced and impact-induced delamination is common in composite structure. The delamination is able to propagate under tensile or compressive stress. Delamination is able to propagate along interface and branch out into next ply. The jumping not only destroys another interface but also creates large stress redistribution, which in some severe condition can break fiber bundles. Thus, the delamination kinking initiation plays an important role on crack jumping between plies. No body has been looking at the delamination kinking initiation affected by manufacturing-induced defects. Once the delamination occurs near the resin-rich area between two plies, as seen in Fig 3, how its extension is affected by voids in the resin-rich area was explored.

### 1.1 Statement of interest

In the current research, a delamination was simulated in a DCB composite specimen subjected to tensile loading. Different shape and size of voids will be located near the delamination crack tip in a resin-rich layer below the delamination. The delamination crack propagation was determined by examining the strain energy release rate (SERR) for delamination extension at different kinking angles. The most energy favorable direction was the kinking direction, as illustrated in Fig 4. Only at interface and angles that kinked into resin were considered. The SERR was evaluated by a revised Virtual

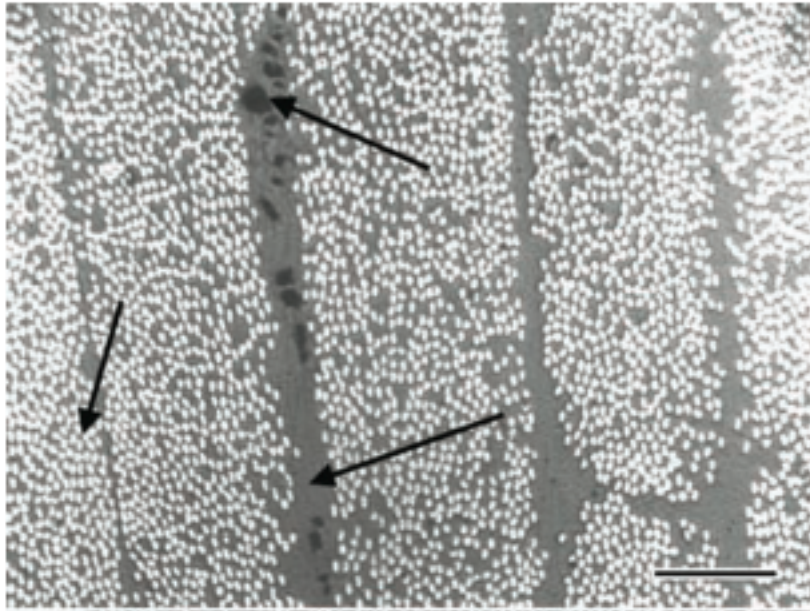
Crack Closure Technics (VCCT) and mixed-mode fracture criterion was applied.



*g. 1: Voids located between plies in prepreg laminates*

(a) Large voids in prepreg laminates

Fig 3 Resin-rich area between plies and voids illustration. [13, 14]



(b) Voids in resin reach area for composites manufactured by autoclave

Fig 3 Continued.

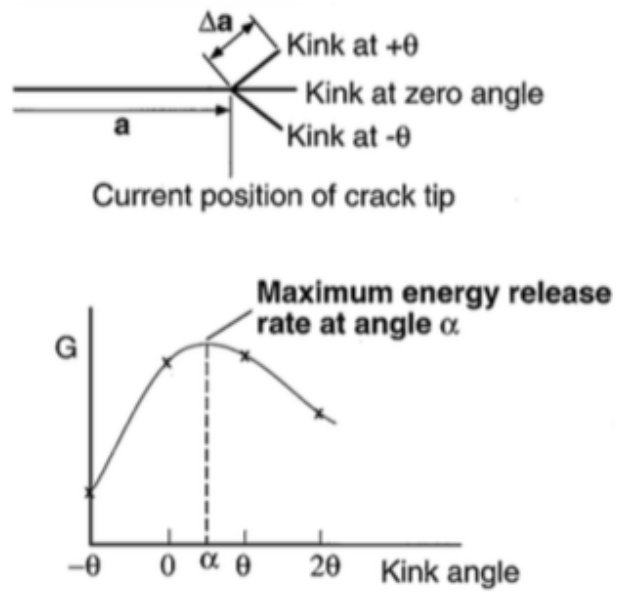


Fig 4 Delamination prediction by examining SERR at different kinking angles[15]

## 2. NUMERICAL INVESTIGATION ON DCB DELAMINATION KINKING WITHOUT MANUFACTURING DEFECTS

In order to quantitatively understand how voids affect delamination crack kinking, different shape, size and distribution of voids were placed near the crack tip. The SERR was calculated for each kinking angle. By applying a fracture criterion based on SERR, it is assumed that damage occurs when it reaches the critical condition. From the energy result, we are able to relate fracture to kinking angles under the influence of different voids and further predict the most favorable crack curving directions.

### 2.1 Characterization of DCB delamination kinking model

Production defects such as large area of delamination inherent in composites and in-service damage like impacted induced delamination are two common kinds of interlaminar fracture in composites. Delamination in composites can propagate in tensile or compressive loading. In order to clarify the mechanism of manufacturing induced defects on delamination kink-out under tensile loading condition, a delamination crack-kinking problem in a DCB model without voids has been first simulated in 2D condition. In tensile loading, the performance of the delamination crack propagation was

studied and examined.

The double cantilever beam (DCB) is widely used for testing delamination resistance under various loading conditions. In the current model, a 2D DCB specimen with cross-ply layup was modeled and loaded with equal tensile force in front of DCB arms. Considering the existence of the resin-rich region between adjacent plies, a thin homogeneous resin layer has been inserted between the middle  $90^\circ$  and  $0^\circ$  plies. Different from the resin interlayer method which places the delamination crack within the thin resin layer[16], the interface crack is located between an upper  $90^\circ$ -ply and the resin layer. The reason of doing so is that before the interface crack extends into neighboring fiber ply, the thin resin-rich area is where the crack first kinks. This area can be relatively thick and should not be ignored. The influence of resin area on kinking should be first studied. In addition, it is convenient and reasonable to put the void in this resin region instead of in fiber ply. The basic geometric properties of DCB model and loading condition are sketched in Fig 5. The thickness of a single ply is assumed as 0.15 mm. The gauge length of the model,  $L$ , equals to 60 mm and with upper arm of 1.65 mm in thickness. The thickness of the lower arm is the total of resin layer  $t$  and composite plies  $t_2$ . An interfacial delamination crack of 25 mm is placed between the middle  $90^\circ$  ply and resin layer. The delamination was modeled as free surfaces. The right end of DCB model is

fixed and tensile forces are applied on the tip of upper and lower arms to activate the interfacial crack. Composite layup, material properties of unidirectional lamina as well as resin are summarized in Table 2 and Table 3.

As described in introduction, in order to study the crack-kinking problem without manufacturing induced defects, a small crack with length of  $\Delta a$  was simulated following the delamination crack in the DCB model. The crack will extend into resin layer and the length is small compared to the interfacial delamination crack. The angle between the delamination plane and kinked crack is characterized as a positive clockwise angle  $\theta$ .

The geometry of kinked crack is sketched in Fig 6.

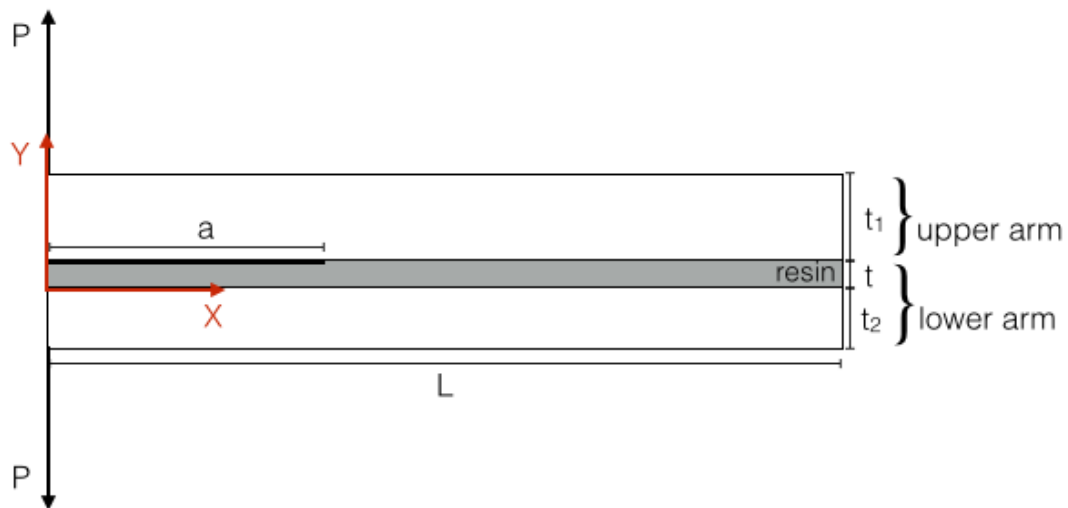


Fig 5 DCB delamination model illustration

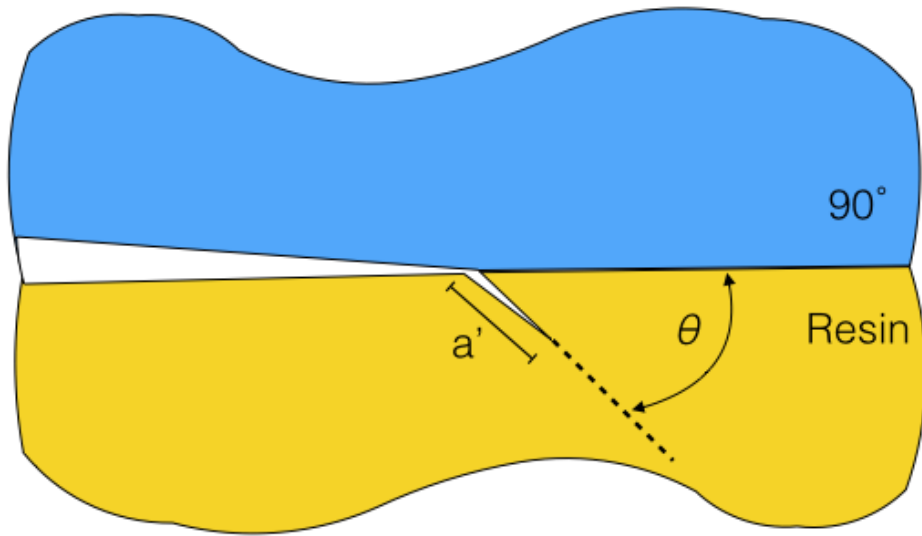


Fig 6 Crack kinking illustration in front of delamination crack tip.

Table 2 Material constants [2]

Unidirectional Lamina	$E_1$ /GPa	$E_2$ /GPa	$E_3$ /GPa	$G_{12}$ /GPa	$G_{13}$ /GPa	$G_{23}$ /GPa	$\nu_{12}$	$\nu_{13}$	$\nu_{23}$
	160	11.38	11.38	5.17	5.17	3.92	0.45	0.32	0.32

Table 3 Material constants of homogeneous resin [3]

resin	Young's modulus /GPa	Poisson's ratio
	2.4	0.3

Table 4 DCB geometric properties and composite layup

L/ mm	a / mm	$t_1$ / mm	$t_2$ / mm	a'/mm	P/N
60	25	1.65	1.35	0.05	65
Composite layup	upper arm		lower arm		
	(0/90) <sub>5</sub> /90		resin + (0/90) <sub>4</sub> /0		

## 2.2 Finite element model illustration

The prediction of delamination crack kinking problem involves two important aspects: one is when the crack starts kinking and the other is in what direction the crack kink out. Several approaches can be applied to solve the first problem. One of the classical methods is to explore the stress intensity factor and compare with critical K values. Except for that, estimating the SERR for mode I and mode II and compare them with critical G values is another commonly used method. Based on the geometry of DCB model given above, the numerical model of delamination crack kinking is simulated in a commercial finite element analysis (FEA) software Abaqus<sup>®</sup>. Considering the following two reasons, the energy criterion is selected in current damage evaluation. First, the delamination crack is between an orthotropic 90-degree ply and a homogeneous resin layer. Abaqus<sup>®</sup> can only give accurate stress intensity factors for isotropic bi-material interfacial crack [17]. Second, the calculation of J-integral in Abaqus has more accuracy owing to the area integral rather than a line integral [18]. Base on these, implementing the calculation through energy criterion can give results that are more reliable.

Crack is assumed to extend in most energy favorable direction. The interfacial crack propagates in mixed-mode owing to the dissimilar materials as well as geometric

asymmetry of upper and lower arms. Even though the contact zone ahead of the bi-material interfacial crack makes it a mixed-mode fracture, when the size of the contact zone is extremely small [19] compared with crack length or adjacent layer thickness, the effect can be ignored and the linear elastic model is adequate. In addition, according to analysis of Ming-Yuan He and John W. Hutchinson [20] on isotropic interface crack kinking, the opening of the kinked crack is less likely affected by contact between crack faces. Linear fracture mechanics is applied in damage analysis.

### 2.3 Two-step revised VCCT

In order to evaluate the crack propagation through energy criterion, a revised VCCT is applied in the analysis[21]. This method is able to separate the energy rate for Mode I and Mode II fracture effectively. When the crack is geometrically asymmetric, like crack kinking in this problem, the normal and shear stresses will couple and create difficulty on mode separation[9]. The revised VCCT can eliminate the coupling between stresses by close the crack in two separate steps and give accurate results for Mode I and Mode II SERR.

Step I: After the crack propagates, the displacements at crack tip with respect to  $x$  and  $z$

direction are illustrated in Fig 7. To apply the revised VCCT, first, the open in z direction will be closed, considered as the Mode I contribution, seen in Fig 8(a). The load  $Z_C^{(I)}$  corresponds to the stress that closes displacement  $\Delta\omega_C$  in Z direction. When the crack is closed along z direction, a null force,  $X_C=0$ , is applied at C to make sure mode purity. However, due to the coupling, the crack open in X direction will be affected and the amount is characterized as  $\Delta u_C$ .

Forces and displacements in Step I:

$$X_C^{(I)}=0 \quad (2.1)$$

$$Z_C^{(I)}=\frac{\Delta\omega_C}{f_{zz}} = \frac{f_{xz}}{f_{zz}}X_C + Z_C \quad (2.2)$$

$$\Delta u_C^{(I)} = f_{xz}Z_C^{(I)} = \frac{f_{xz}}{f_{zz}}\Delta\omega_C \quad (2.3)$$

$$\Delta\omega_C^{(I)} = f_{zz}Z_C^{(I)} = \Delta\omega_C \quad (2.4)$$

Step II: The residual crack open  $\Delta u_C^{(II)}$  in x direction is closed by applying stresses  $X_C^{(II)}$  and  $Z_C^{(II)}$  in x and z direction. The crack is recovered back to the state before extension, seen in Fig 8(b). This crack closure corresponds to crack sliding, which is a Mode II fracture process.

Forces and displacements in Step II:

$$X_C^{(II)} = X_C \quad (2.5)$$

$$Z_C^{(II)} = Z_C - Z_C^{(I)} = -\frac{f_{xz}}{f_{zz}} X_C \quad (2.6)$$

$$\Delta u_C^{(II)} = \Delta u_C - \Delta u_C^{(I)} = \left( f_{xx} - \frac{f_{xz}^2}{f_{zz}} \right) X_C \quad (2.7)$$

$$\Delta \omega_C^{(II)} = 0 \quad (2.8)$$

By separating the crack closure into two steps: close and slide, the mode contribution can be summarized in the equations:

$$G_I = \frac{Z_C^{(I)} \Delta \omega_C^{(I)}}{2\Delta a} \quad (2.9)$$

$$G_{II} = \frac{X_C^{(II)} \Delta u_C^{(II)}}{2\Delta a} \quad (2.10)$$

Based on an assumption that the energy required to extend the crack from  $a$  to  $a+\Delta a$  equals to the energy needed to close the crack of length  $\Delta a$  [22]. A symmetrical uniform element is adopted around the crack tip. Same element was used in interface crack and kinked crack, as seen in Fig 9. The size of the element is characterized as  $e$  and mesh refinement has been applied to ensure the accuracy of SERR. Eight-node plane strain quadrilateral reduced integration elements (CPE8R) were adopted and elements around crack tip are well meshed.

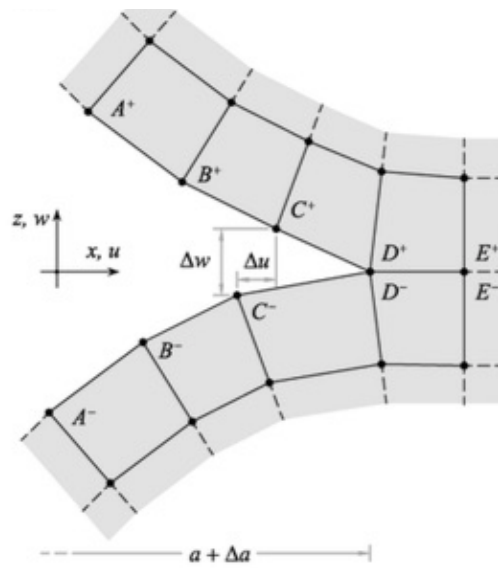


Fig 7 Crack open displacements in x and z direction after crack extends  $\Delta a$

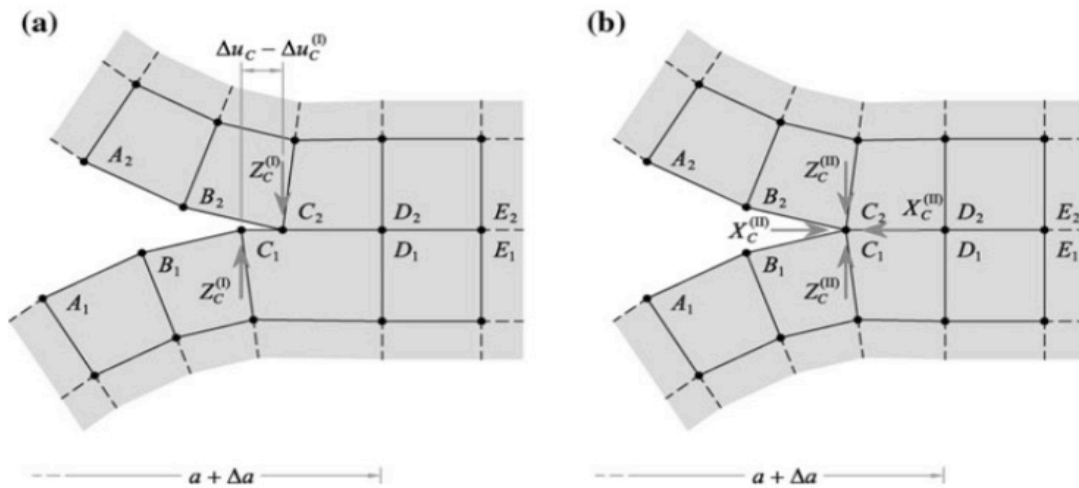
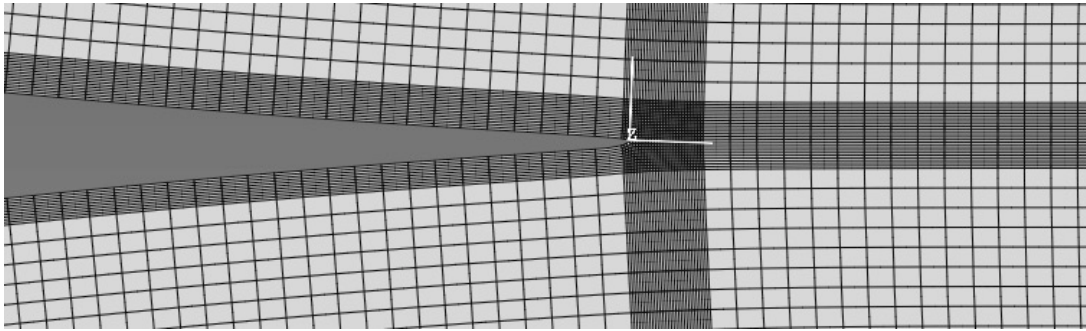
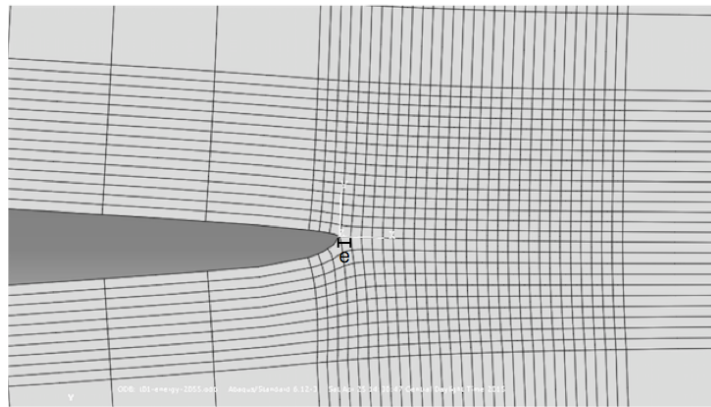


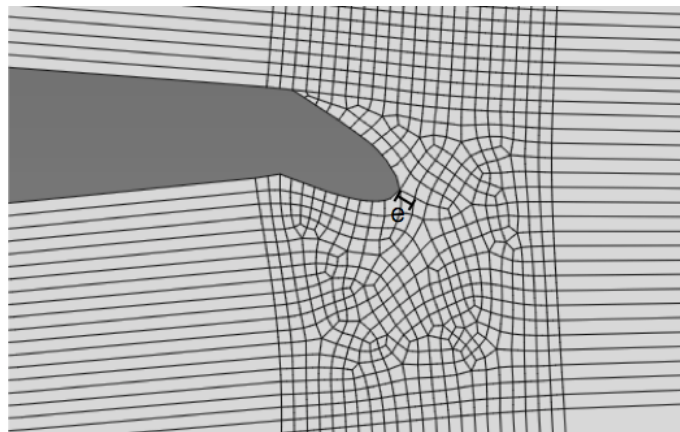
Fig 8 Two steps crack closure. (a) closing the open in z-direction, (b) closing the open in x-direction



(a) DCB crack open



(b) Finite element in front of interface crack tip



(c) Finite element around the kinked crack tip

Fig 9 Finite element illustration around crack tip

## 2.4 Mesh refinement and FE validation

The FE model validation was done by comparing the SERR got from revised VCCT and embedded J-integral in Abaqus. Different FE sizes around crack tip were applied for purpose of getting convergence value of  $G$ . The thickness of resin layer  $t$  equals to 0.1 mm as an example. Several contours surrounding crack tip were evaluated to get J-integral and the discrepancies between each contour were small until J-integral approaches constant.

Total SERR based on revised VCCT as well as J-integral was obtained and plotted in Fig 10. The element size was modified from 0.001 mm to 0.01 mm. From the result, the J-integral is independent of element size as each contour reached its saturation value.

The  $G_I$  and  $G_{II}$  gradually become convergence with increasing element size. The reason for the variation is that when element size is small, the evaluation of SERR by VCCT could include some stress oscillation around crack tip. The element length, as suggested in [22], should be small enough to converge FE solution but large enough to avoid the oscillating results. To avoid the stress oscillation and have reliable simulation at the same time, element size  $e$  is chosen as 0.01 mm in the following study.

With constant FE meshing, the SERR correspond to different kinking angle were calculated by revised VCCT and J-integral. The results were compared in Fig 11. With increasing kinked angle, total SERR decreases. The maximum disparity between revised VCCT and J-integral is as small as 5.9% of J-integral.

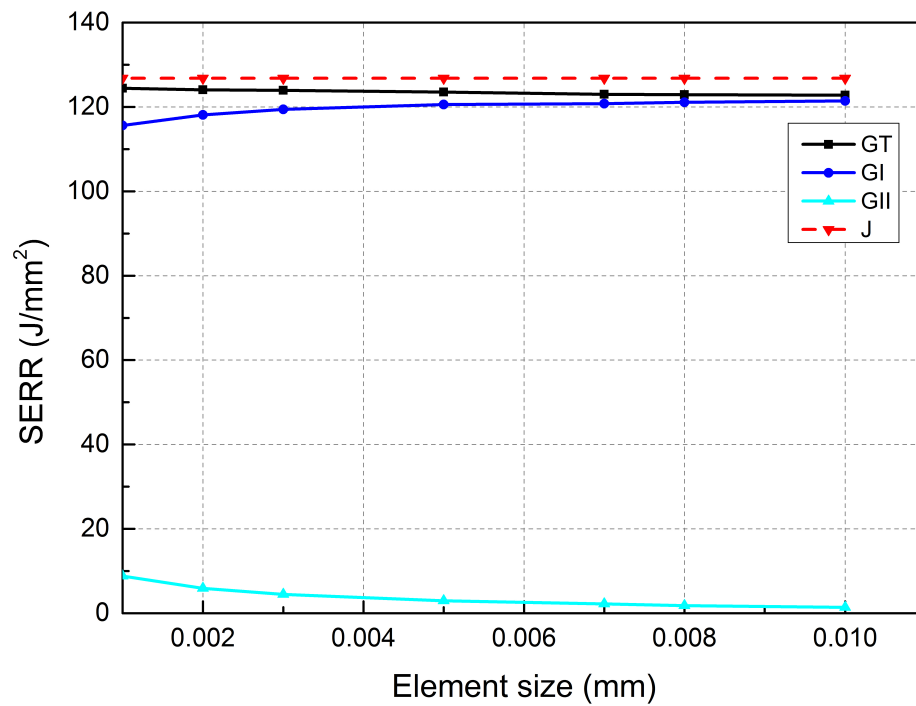


Fig 10 SERR convergence with element size

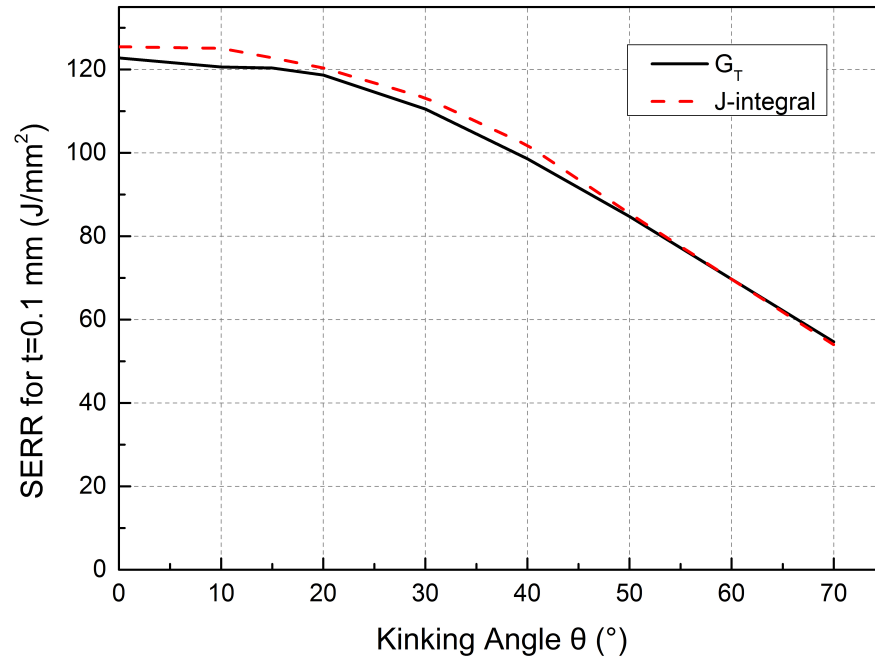


Fig 11 Model examine by comparison of J-integral and total SERR

## 2.5 DCB delamination crack kinking analysis

The problem of DCB delamination crack kink out in tensile loading was studied with several different resin thicknesses. The general deformation of kinked crack is illustrated in Fig 12. From the shape of crack open, it is clear that the small crack extended into resin layer can hardly affect the main delamination crack surface. At different kinked direction, the SERR for Mode I and Mode II fracture were calculated with respect to kinking angles  $\theta$ . For instance, when the resin thickness equals to 0.1 mm, the variation of  $G_I$  and  $G_{II}$  with respect to kinking angle are plotted in Fig 12 and ratio between  $G_I$  and

$G_{II}$  in Fig 13. With gradually increasing kinking angle, the Mode I SERR descends while Mode II SERR falls initially and rises again. From the ratio of  $G_{II}$  and  $G_I$  as well as their values, the kinked crack extension is always in mixed-mode and governed by Mode I crack open, especially at small kinking angles. The equal tensile loadings and nearly symmetric DCB arms determine that the crack extends in Mode I dominated manner. With larger kinking angles, crack open in Mode I becomes difficult because of the curved crack geometry, while Mode II crack extension become possible by crack surfaces sliding. Limited by the curved crack shape and small crack extension, the Mode II crack was also constrained.

The 2-D mixed-mode fracture criterion based on SERR is assumed to be in the following form [23]:

$$\left(\frac{G_I}{G_{IC}}\right)^m + \left(\frac{G_{II}}{G_{IIC}}\right)^n = 1 \quad (2.11)$$

Where  $m$  and  $n$  are constants which determine the contribution of Mode I and Mode II to the fracture process. Because the values of these constants above are obtained mostly from experimental data fitting, it was assumed here that  $m$  and  $n$  equal to two in this simulation.

$$C = \left(\frac{G_I}{G_{IC}}\right)^2 + \left(\frac{G_{II}}{G_{IIC}}\right)^2 = 1 \quad (2.12)$$

The critical  $G_I$  and  $G_{II}$  for resin are assumed to be 120 GPa and 760 GPa [24]. The left-hand side of the mixed-mode criterion above is characterized as a parameter  $C$  and the fracture was investigated at different kinking angles. From results in Fig 14, the delamination crack would only propagate along interface rather than kinking into resin layer.

As a mixed-mode DCB fracture under the tensile loading, the asymmetry of upper and lower arm introduces a crack kinking probability. By the same process, several models with resin layer of different thickness were simulated. The  $G_I$  and  $G_{II}$  are summarized in Fig 15. One of the common feature as in  $t=0.1$  mm condition is that the fracture process is Mode I dominated. Values of  $G_{II}$  are small and mode II crack open does not control the fracture even at large kinked angles. When the mixed-mode fracture criterion was adopted, as seen in Fig 15, the potential kinking angle varies with resin layer thickness. The most favorable kinking direction is the one which has maximum  $C$  value. With very thin resin layer, such as  $t = 0.075$  mm, the delamination is trapped at interface, nevertheless, with very thick resin, such as  $t=0.5$  mm the crack will kink at around 20 degree. When the resin area is thick, the interface fracture is constrained and crack

extends into resin.

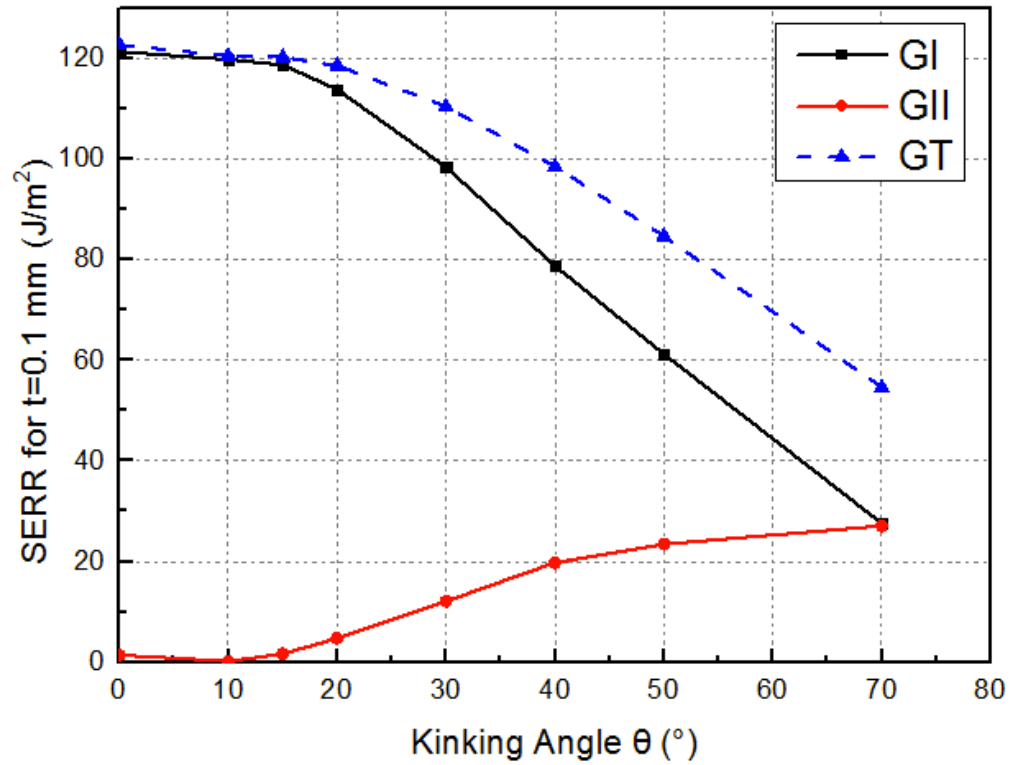


Fig 12 SERR for Mode I and Mode II when resin thickness  $t = 0.1$  mm, no void

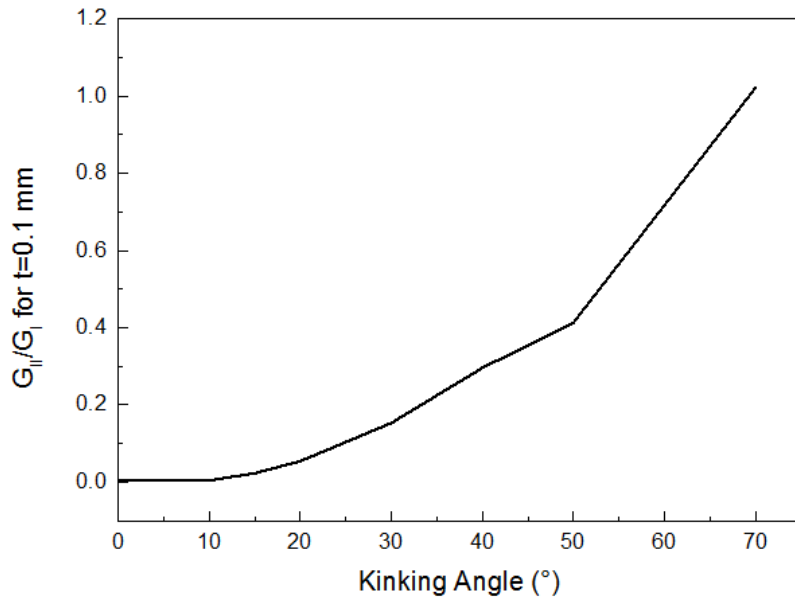


Fig 13 Mode mixity for resin  $t=0.1$  mm, no void

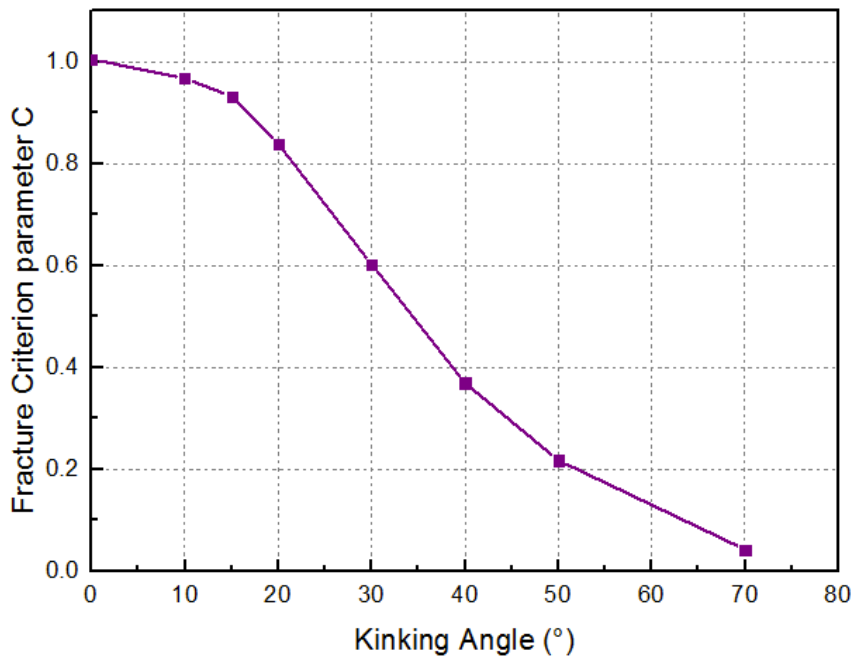


Fig 14 Fracture criterion parameter C with respect to kinking angles when resin  $t=0.1$

mm

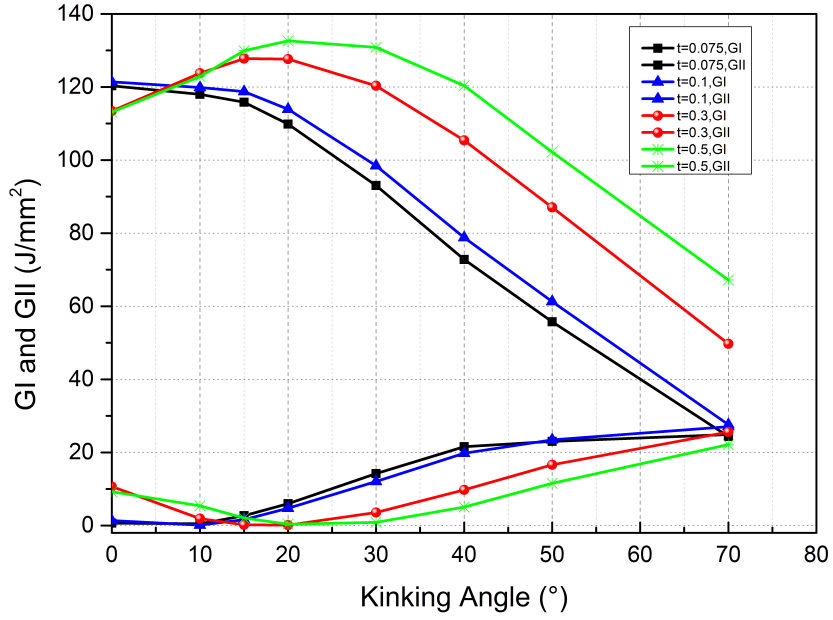


Fig 15 SERR for different resin thickness, no void

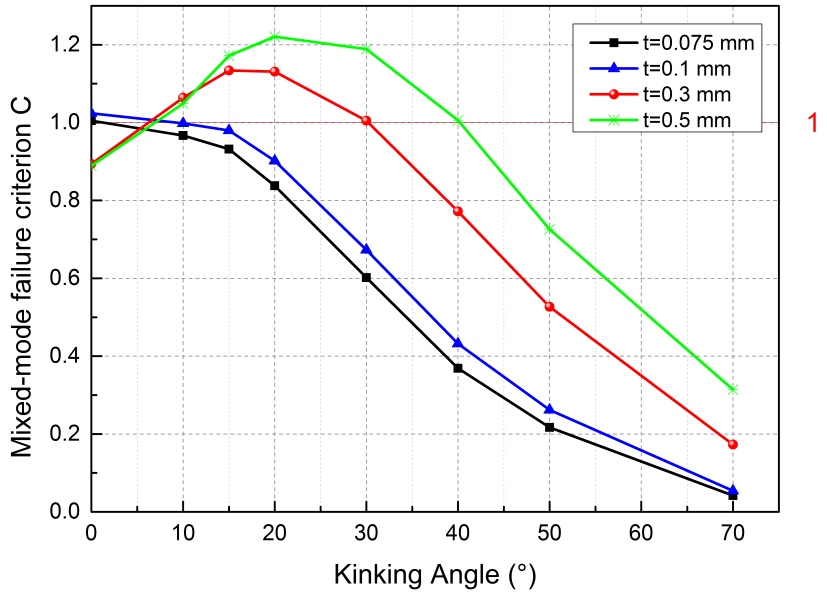


Fig 16 Values of fracture criterion with different thickness resin layer

## 2.6 Summary

In this section, composite delamination problem under tensile loading without voids was examined. After simulation, it has been found out that:

- (a) Considering the asymmetric of DCB specimen and crack surface, delamination propagates in mixed-mode.
- (b) The mixed-mode delamination extension is Mode I dominated when kinking angle is small. At larger kinking angles, Mode I and Mode II crack open become competitive.
- (c) Delamination in thinner resin layer would be constrained in interface. In thick resin DCB specimen, such as  $t = 0.3$  mm, delamination is able to kink and the potential kinking direction is positive related with resin thickness. The maximum kinking angle is 20-degree when  $t$  equals to 0.5 mm.

### 3. NUMERICAL INVESTIGATION ON DCB DELAMINATION KINKING WITH MANUFACTURING VOIDS IN RESIN-RICH LAYER

In this part, the delamination crack kinking problem was explored with the presence of voids in resin layer. A 2D DCB model was built with keeping all modeling conditions in the previous section. The resin thickness was chosen as 0.1 mm for reason that the delamination will extend along its original path without any influence from defects. By simulation of voids in resin layer, the problem of delamination kinking was investigated.

#### 3.1 Characterization of manufacturing defects in FE simulation

In introduction, the morphology and distribution of voids in composites were well discussed and summarized. In the following study, both circular and elliptical shape voids were explored. Limited by the thickness of resin-rich layer, the maximum radius of circular void is 30  $\mu\text{m}$ . In composite, the distribution and size of voids are two possible factors that can affect composite performance. As stated in [11], voids can affect composite fracture when located at more critical position. In addition, from the research about interaction between void and Mode I delamination crack by Mauro Ricotta[25], it

should be noticed that the influence of void on crack extension are effective when the distance between crack tip and void is small. As a result, in the following simulation, various shapes and sizes of voids were placed in resin-rich layer near the delamination crack tip. The distance between crack front and void varies for purpose of investigating effect of void location on crack kinking.

The schematic diagram in Fig 17 depicts the location of voids in resin layer. The horizontal distance from the void center to delamination crack tip is characterized as  $d$ . The vertical distance from void center to delamination plane is assumed to be 40 micrometers. As a parametric study of voids on crack kinking, the possible shapes of resin voids must be taken care of. Several experimental observations [16] show that small circular or elongated cigar-shape voids are common in composites. In the 2-D FE model, both circular and elliptical voids near crack tip are considered and their shapes are illustrated in Fig 18. The materials at the location occupied by voids were taken out. Circular and elliptical voids are characterized as radius  $R$ , major axis  $L_a$  and minor axis  $L_b$  respectively.

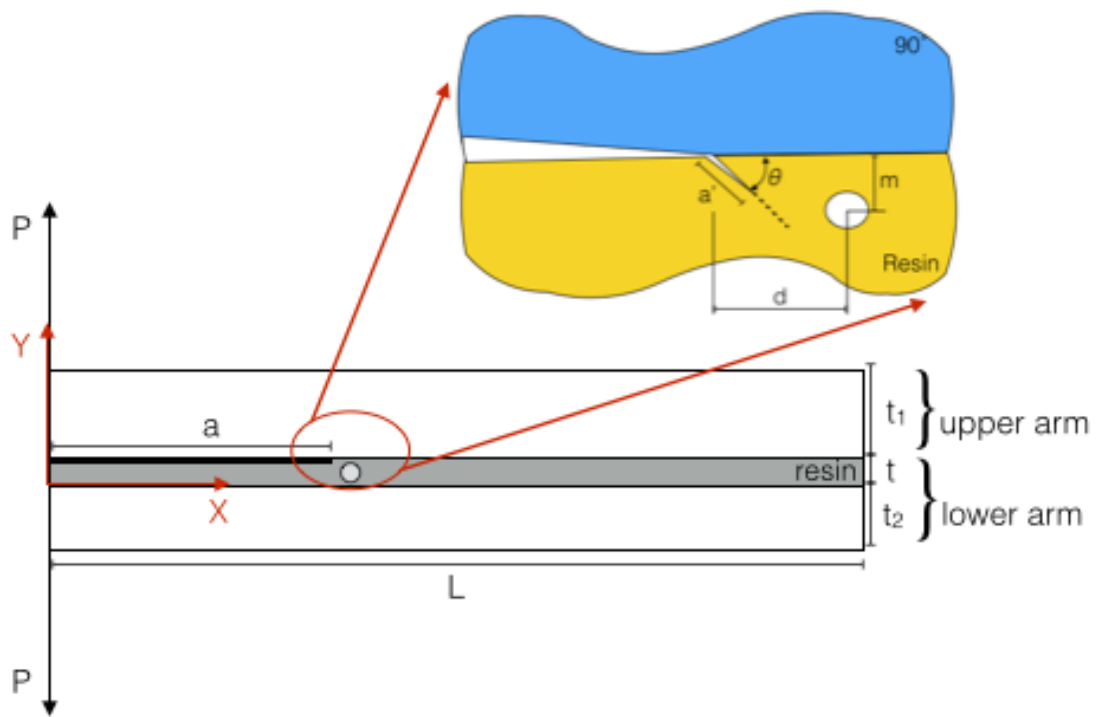
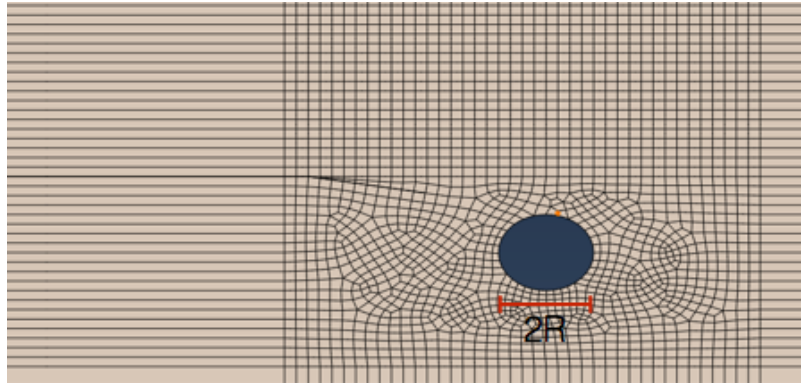
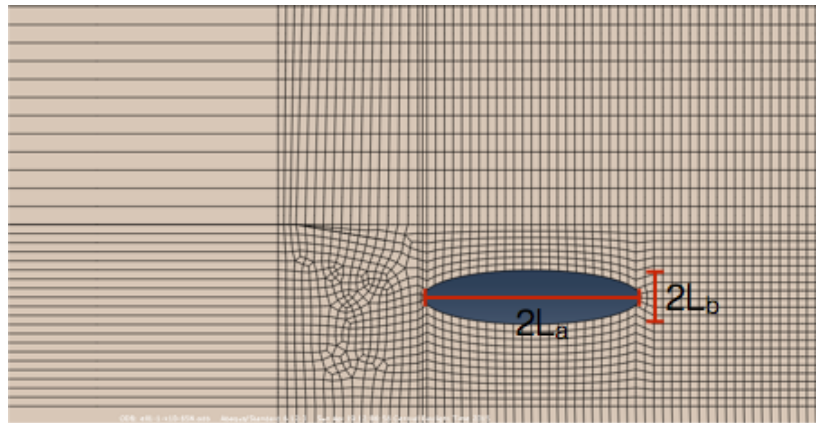


Fig 17 Illustration of DCB model with void



(a) Circular void at crack front



(b) Elliptical void at crack front

Fig 18 FE illustration of voids

### 3.2 Quantified study of voids on delamination crack kinking

#### 3.2.1 Effects of circular voids on crack kinking

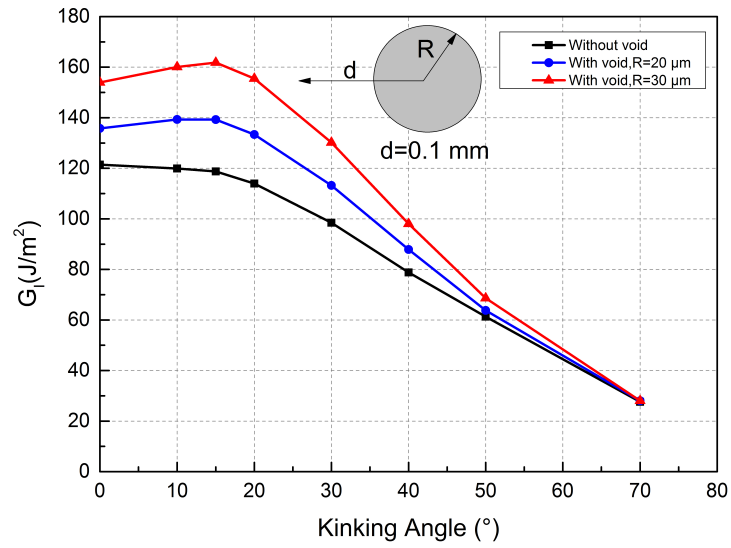
As illustrated above, FE model was built with presence of circular voids near delamination crack. Sizes of voids are modified by changing void radius,  $R$ . The values of Mode I and Mode II SERR are evaluated with resin voids at several locations. When

the horizontal distance between void center and delamination crack tip,  $d$ , equals to 0.1 mm, the effects of void on  $G_I$  and  $G_{II}$  are depicted in Fig 19. The existence of voids near crack tip has more effects on Mode I crack open; especially when crack kinks within 30 degree. The experiment on examining critical value for Mode I and Mode II delamination crack open shows that  $G_{II}$  is relative insensitive to composite porosity compared with  $G_I$ . By applying mixed-mode SERR criterion, crack kinking angles can be evaluated. The results of fracture criterion  $C$  at each kinking angle are plotted in Fig 21. When there is no void at resin area below the delamination, based on the criterion, delamination would propagate along interface plane. When voids are distributed around the delamination, from Fig 21, the angle with respect to maximum  $C$  is not at 0-degree any more. The result implies that delamination is able to kink out from interface plane. In addition, the potential kinking angle is determined by radius of circular void. When a circular void with 30-micrometer radius was considered, crack kinks around 15 degrees. With void's radius equals to 20 micrometer, crack kinks at about 10 degrees. Larger void causes more stress perturbation at crack tip and

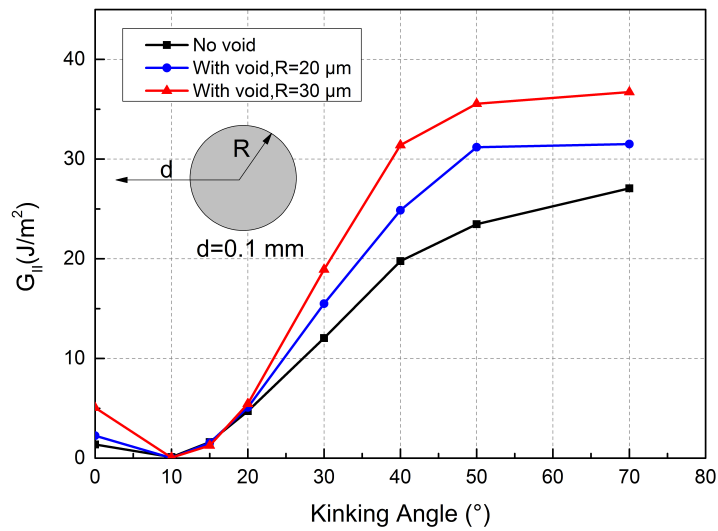
Except for the size of circular void, effects of distance between void and crack tip were also investigated. By placing circular voids at different location, the influence of void on each possible crack kinking directions was discussed, as seen in Fig 21. For the reason

that voids have more effects on Mode I SERR and the failure is Mode I dominated, it is more important to look at how  $G_I$  is affected by voids. From the comparison, the presence of circular void increases  $G_I$  at all kinking angles.  $G_I$  at 15-degree with larger void was affected most. The value is over 1.4 times of the case without void. The influence diminishes when voids are 1 mm away from crack tip. The mixed-mode failure criterion was applied and C values are plotted in Fig 20. From Fig 20(a) and (b), it is clear that at the same loading condition, the void makes delamination propagation easier in all discussed directions compared with no void case. The larger the size of circular void is, the less effort needs to advance the crack. The gauge distance of benefiting crack extension is about 0.5 mm. What's more important; the void located within 0.2 mm away from crack tip attracts the crack and curves it into resin layer. The maximum kinking angle is 15 degrees.

Larger void introduces more stress oscillation at the crack tip. Compared with the case that no void was considered, the kinking of delamination crack caused by void introduced stress redistribution at crack tip was proved by the results.



(a)



(b)

Fig 19 (a) Size of circular voids and  $G_I$  (b) Size of circular voids and  $G_{II}$

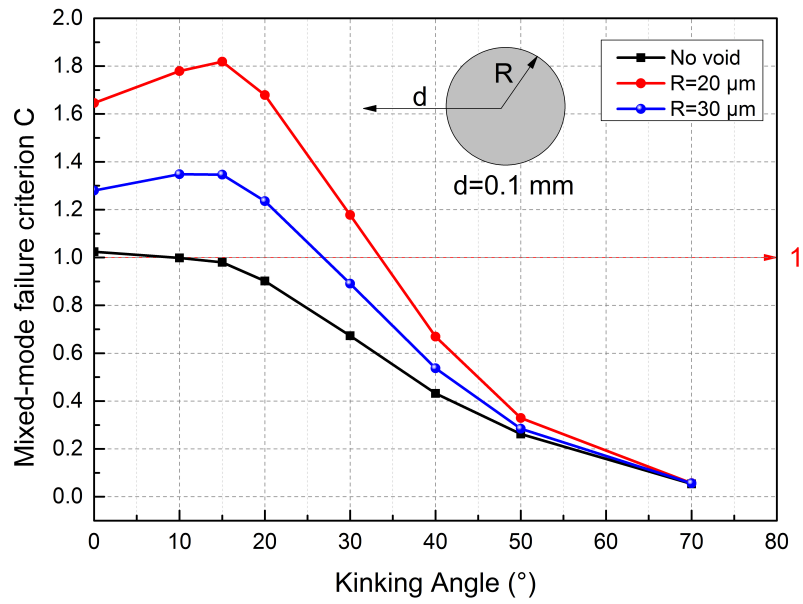
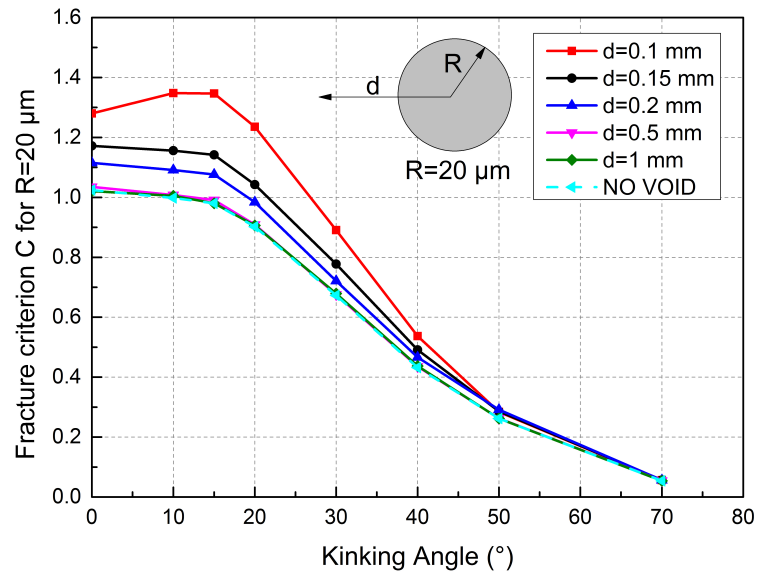
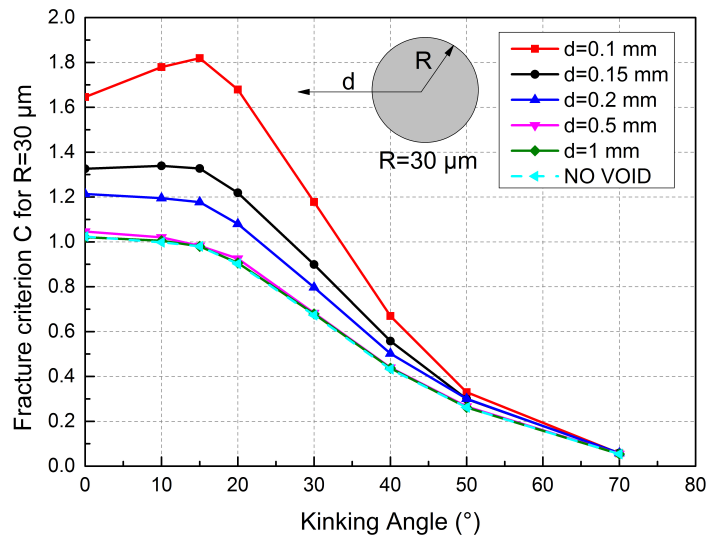


Fig 20 Size effect of circular void on crack kinking



(a)



(b)

Fig 21 Effect of distance of circular void when R=30 μm on crack kinking

### 3.2.2 Effects of elliptical voids on crack kinking

Similar with the FE model of circular void, several shapes of elliptical voids have been simulated to study the shape effects on delamination crack kinking. The geometric parameters of elliptical voids are illustrated in Fig 18 (b). The ratio between major axis and minor axis is elliptical shape parameter. From the simulation results of  $G_I$  and  $G_{II}$ , it has been found that, same as circular voids, crack propagates in Mode I dominated mixed-mode and the existence of elliptical voids have major influence on Mode I SERR in all potential kinking directions. The variation of  $G_I$  has been showed in Fig 22.

Elliptical voids of two sizes were considered. At the same location, the different void sizes have no significant effects on  $G_I$  at each kinking direction. Voids located within 1 mm from crack front can affect Mode I crack open. Meanwhile,  $G_I$  for 15-degree kinking direction was affected most.

Mixed-mode fracture criterion was also applied for elliptical voids to evaluate crack kinking. As seen in Fig 22,  $G_I$  at 15-degree was extremely affected by elliptical void when the distance between void and crack front is small. Therefore, based on Fig 23, the most possible kinking angle is around 15-degree when  $d$  equals to 0.13mm. In addition, the potential kinking angle is not fixed to 15-degree. When the elliptical void was moved

away from crack tip, the most possible kinking angle descends to 10-degree. The delamination becomes a smooth curved crack that extends into resin layer. When elliptical void is moved away from crack front, delamination would be constrained in its original plane. Therefore, the simulation shows that the effective crack kink-out distance between elliptical void and crack front is about 0.2 mm.

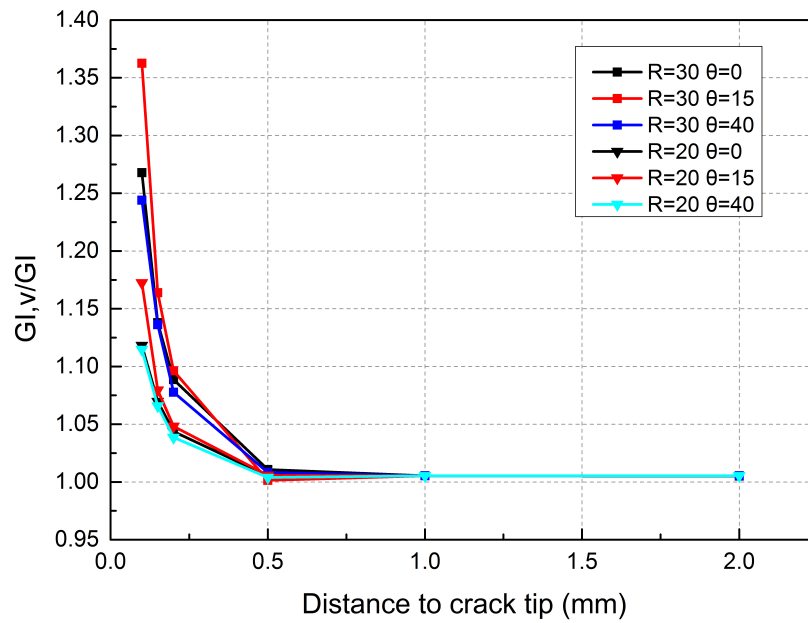


Fig 22 Mode I SERR increased by elliptical void compared with no void.

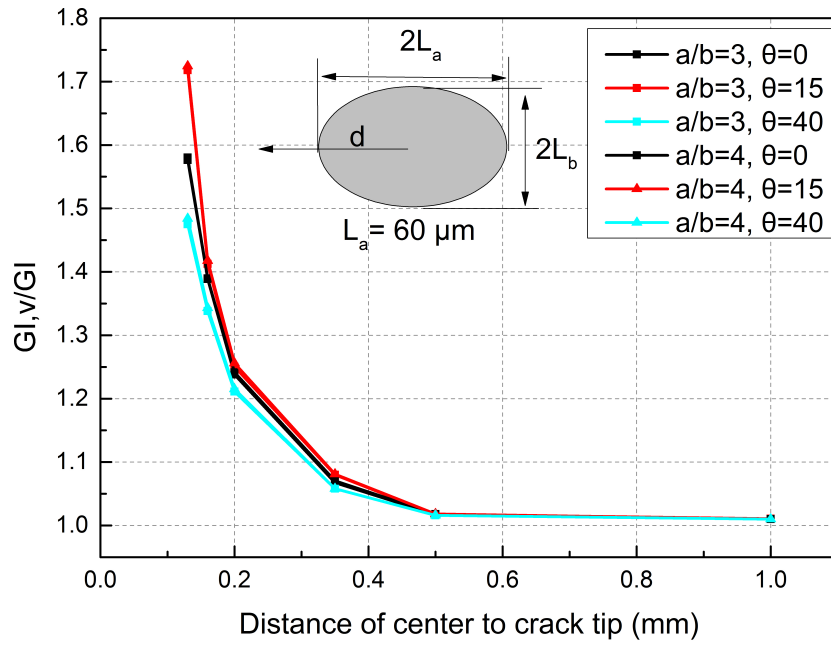


Fig 23 Effects on elliptical void on Mode I SERR at different kinked angle

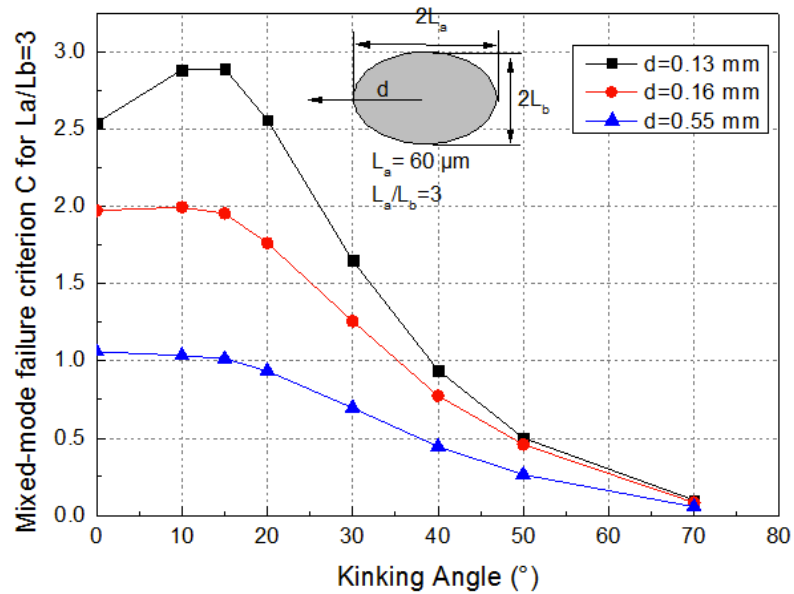


Fig 24 Size effects of circular void on crack kinking

### 3.2.3 Effects of voids with same area on crack kinking

On the basis of previous study, it is clear that the size and shape are main factors of delamination jumping. Further exploration was performed with respect to different void shapes on crack kinking. As depicted in Fig 25, voids placed in front of delamination occupy the identical physical area. It equals to  $900\pi \mu\text{m}^2$ . The distance between delamination tip and crack front,  $d$ , was constant and assumed as 0.1 mm. The only difference between voids is their shape parameter, which characterized as the ratio between major and minor axes.

By applying the mix-mode fracture criterion, fracture parameter  $C$  was plotted with respect to continuous kinking angles, as seen in Fig 26. As  $L_a/L_b$  equals to one, that's a circular void, the maximum  $C$  occurs around 15-degree. By increasing values of  $L_a/L_b$ , the results of  $C$  are dramatically improved at each angle and the maximum appears at smaller angle compared with result of circular void. From the simulation, the influences of different shapes of voids on delamination branching are clear. It is more threatening when there is elliptical void around crack tip compared with circular void. The changes of void shape have limited effects on potential kinking angles.

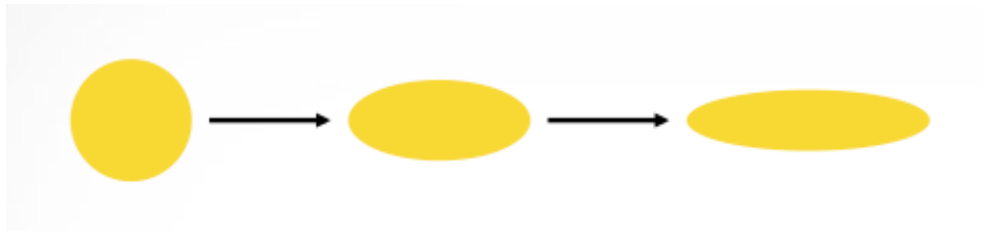


Fig 25 The illustration of voids with same area and different shape parameters

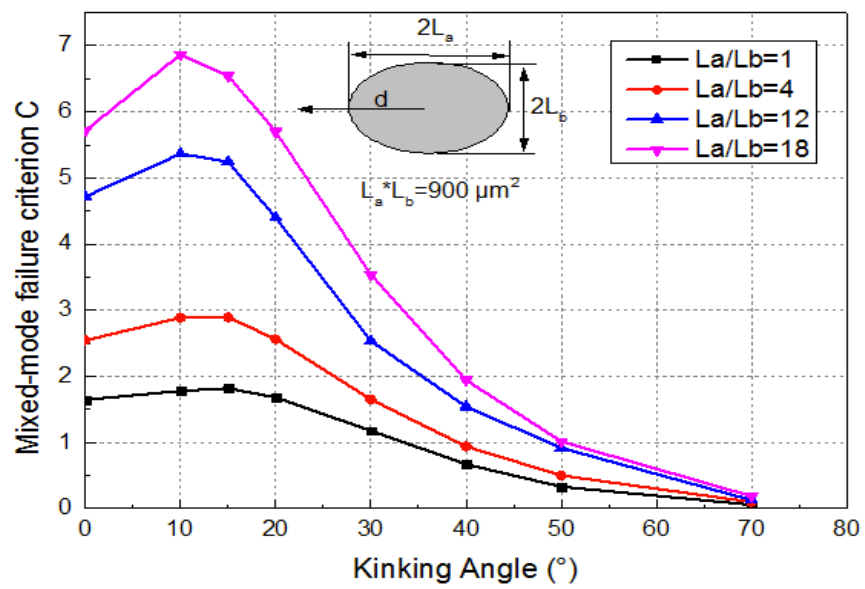


Fig 26 Fracture parameter C for voids of different shapes with respect to kinking angles

### 3.3 Summary

In this section, quantitative study of manufacture-induced voids on DCB delamination crack kinking was carried out. Presence of voids at delamination crack front caused stress perturbation towards voids. Several phenomena have been found out, that:

- (a) Existence of voids of circular and elliptical shapes near crack front increases the value of Mode I SERR. Compared with circular void, elliptical void has more effect on  $G_I$  due to more stress constrain.
- (b) The effective distance for voids to activate delamination kinking is around 0.2 mm. With respect to voids shape, the distance between void and crack tip is more essential on crack kinking.
- (c) The most favorable kinking direction is 15-degree when there are circular or elliptical voids adjacent to crack tip. By increasing distance between void and crack, potential kinking angles descend. Elliptical voids give rise to crack kinking compared with circular voids with same size.

## 4. NUMERICAL INVESTIGATION ON MANUFACTURING VOIDS IN RESIN-RICH LAYER AFTER CRACK KINKED

From previous discussions, the existence of voids near delamination crack tip will introduce stress oscillation and activate a crack kinking. In this section, the crack propagation after triggering from interface and growth within the isotropic resin layer was studied. A DCB delamination specimen with 0.3 mm resin layer was considered. In addition, in order to study the influence of defects on kinked crack propagation, circular void was placed in resin layer. The interaction between void and crack was well investigated.

### 4.1 FE model characterization

Based on the simulation in last part, as for comparison, DCB delamination specimens with and without voids were performed in 2D FE simulation. The thickness of resin layer equals to 0.3mm. In tensile loading, delamination crack would kink out from interface at 15-degree, which was shown in previous discussion. The delamination crack-kinking problem with circular voids was first examined. Because of the increase on resin thickness, a larger circular void with 50  $\mu\text{m}$  radius was placed 0.2 mm

horizontally away from delamination front. In thick resin area, circular voids are preferred in manufacturing. A 0.1 mm precrack was simulated as the kinked crack which extends into resin. Except for the modification on resin thickness and void location, similar FE condition was maintained.

After delamination crack kinks, problems of crack growth in resin layer were investigated. A small crack, following the kinked delamination, of 0.02 mm in length was modeled as the crack propagation. Regular uniform elements of size 0.005 mm were chosen to calculate SERR by revised VCCT. At different crack extension directions, the SERR were evaluated and crack extension was predicted by mixed-mode fracture criterion. The angle between the small extended crack and X-axis is characterized as extension angle  $\theta'$ , which can be seen in Fig 27.

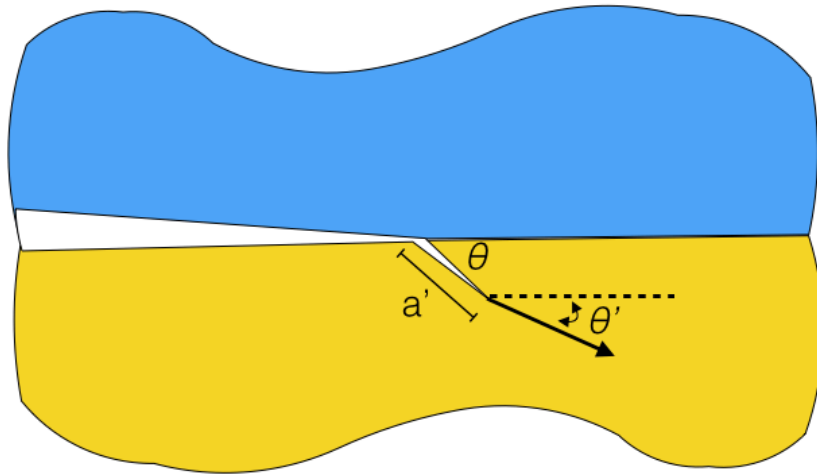


Fig 27 Crack extension illustration

#### 4.2 Effects of circular voids on delamination crack kinking when $t=0.3\text{mm}$

First of all, the influence of circular void with 0.5 mm radius on delamination crack kinking was investigated. Same FE simulation was applied. By taking mixed-mode fracture criterion, the most favorable kinking direction was identified. As depicted in Fig 28, the most possible kinking angle, which has maximum  $C$ , was not affected much by the circular void. Probably it is because with respect to a 0.2 mm effective gauge distance of void on crack kinking, the delamination crack was less affected by current void. The DCB geometry and stiffness of arms are more critical factors which dominate stress state of delamination crack. In consequence, the delamination in cases with and

without void are considered to kink out at 15-degree.

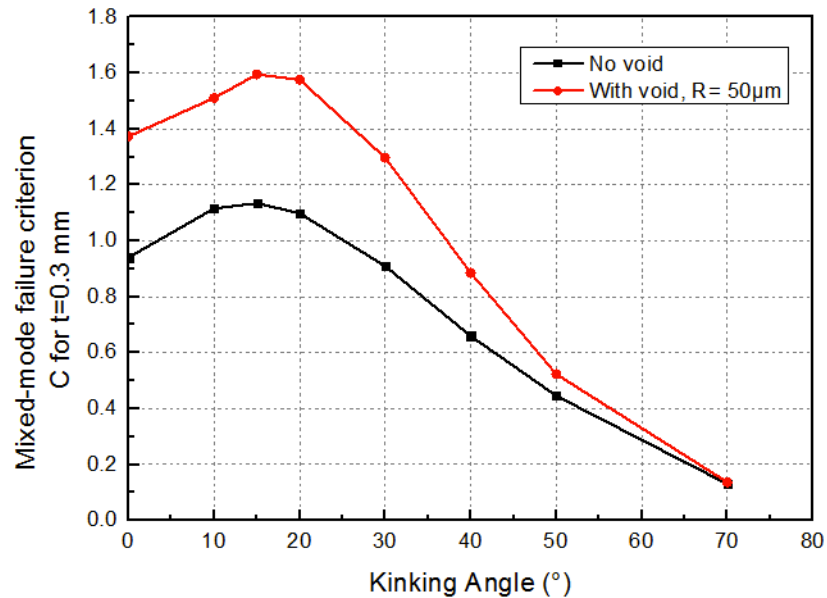


Fig 28 Effect of circular void on crack kinking when t= 0.3mm

#### 4.3 Effects of circular voids on crack propagation within resin layer

After a 15-degree crack kinking, the FE simulation was carried out. First, the crack extension with no influence of void was explored. From Fig 29, the crack growth in isotropic resin layer was in mixed-mode when the extension angle modified from negative 15 to 35-degree. When the extension angle  $\theta'$  was around 12-degree, SERR for Mode II almost diminished. One of the failure criterion widely used in mixed-mode

crack extension requires that crack extends along the direction that  $G_{II} = 0$ . By applying mixed-mode fracture criterion, as shown in Fig 30, crack extends in 12-degree. Without any stress perturbation, the kinked crack does not go at 15-degree but turned a little bit towards the interface. A second crack extension was modeled following the 12-degree crack growth. From the results in Fig 30(b), after a 12-degree extension, crack continue grows along 15-degree. The simulation shows that once crack kinks out at some angle, the geometric condition will constrain the extension even with some small fluctuation.

Crack extension was also examined with present of void. As illustrated in Fig 31, fracture criterion results show that first crack extension was at 16-degree and second extension was at 20-degree. The circular void gradually attracts the crack and turns the its direction. The crack propagation was affected by present of void when crack tip is close enough to it.

#### 4.4 Stress analysis for crack extension with void

As illustrated in Fig 32, stress contour around crack tip was examined. The crack opens at 15-degree and a 180-degree contour was picked. Distortion and Dilatational energy density were investigated and depicted in Fig 33. The contour stars from upper part of

crack tip. In Fig 33, 0-degree stands for the starting of the contour and 180-degree stands for the end of the contour. Critical distortion energy density for epoxy resin is around 1.4 MPa and according to Fig 33 that  $U_d$  is much smaller than 1.4 MPa, crack extension is not a ductile fracture process. The dilatational energy density at crack tip has maximum value at around 95-degree. Considering that 90-degree stands for crack original propagate direction, crack will turn around 5-degree downwards. The results of dilatational energy density meet the prediction based on mixed-mode fracture criterion. Mode I dominated crack propagation in resin is brittle fracture and the direction can be estimated by maximum dilatational energy density.

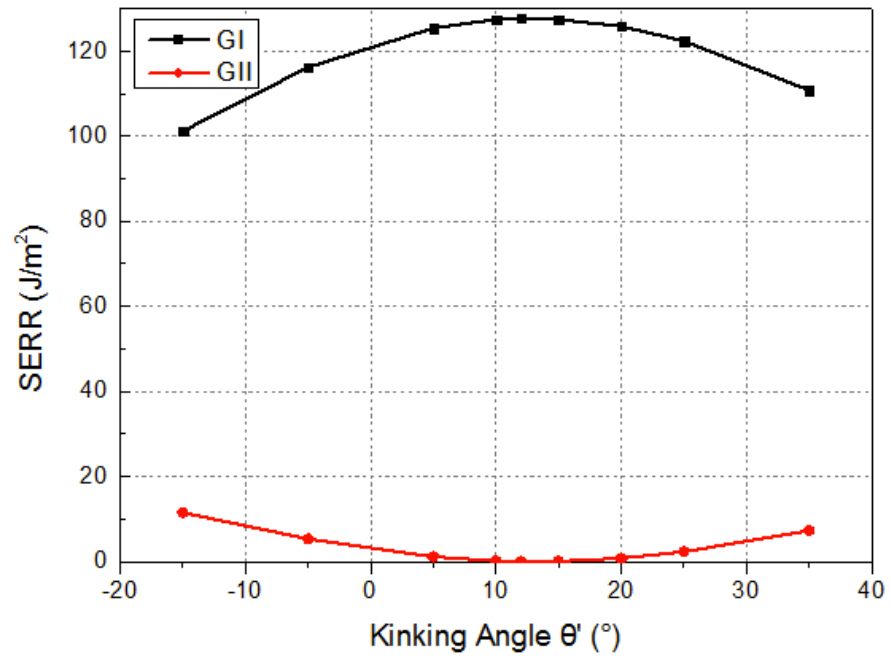
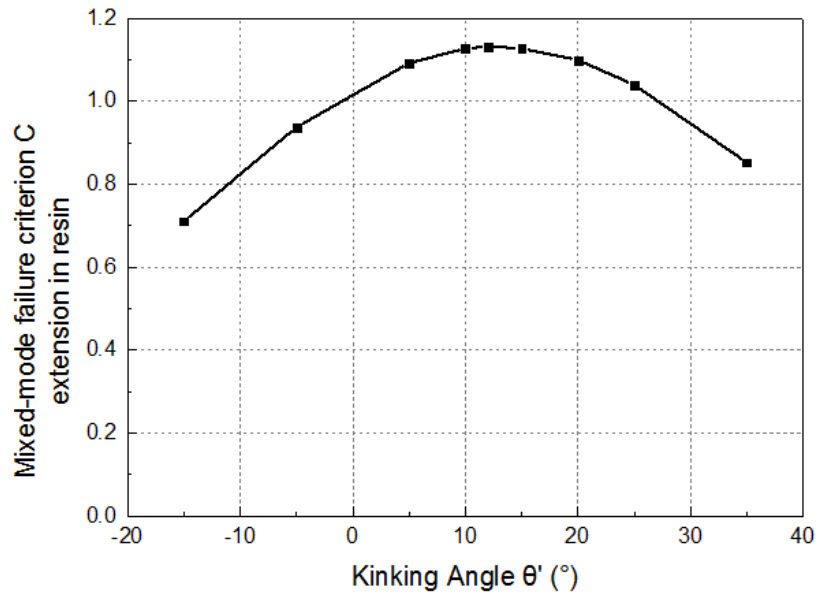
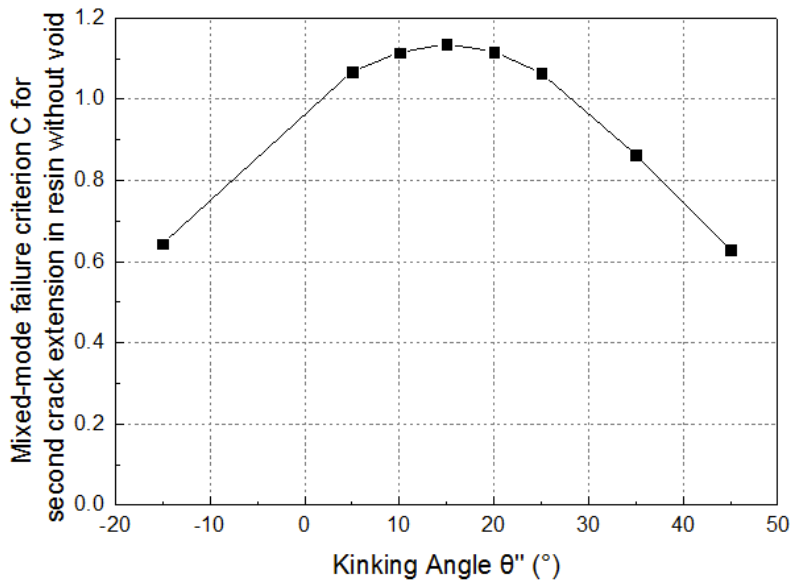


Fig 29 Mode separation of kinked crack

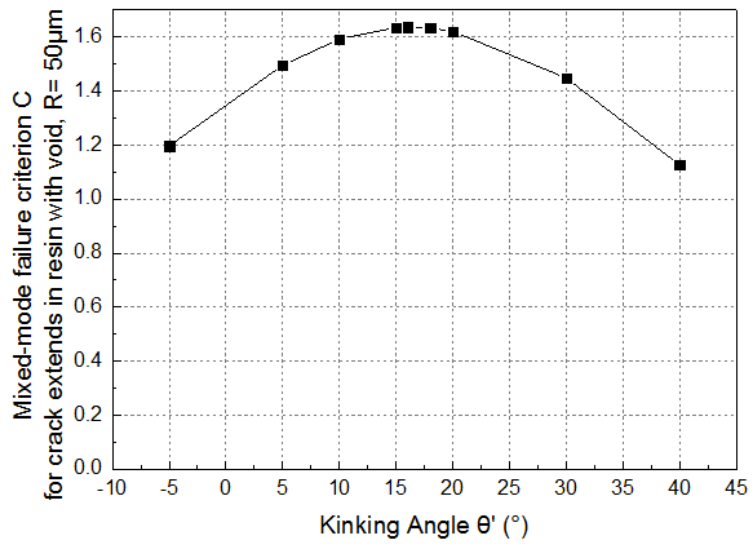


(a) Fracture criterion applied on first crack extension in resin without void

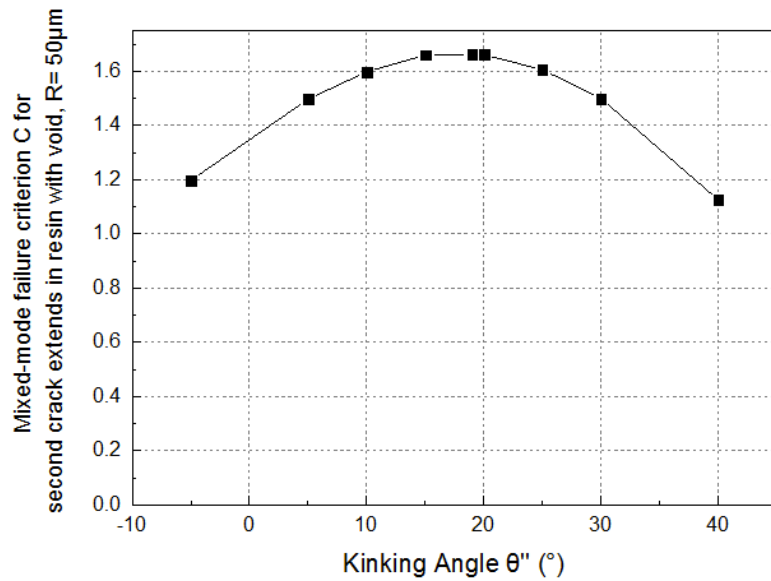


(b) Fracture criterion applied on second crack extension in resin without void

Fig 30 Fracture criterion C for crack extension in resin without void



(a) Fracture criterion applied on first crack extension in resin with void, R=50 µm



(b) Fracture criterion applied on second crack extension in resin with void, R=50 µm

Fig 31 Fracture criterion C for crack extension in resin with void

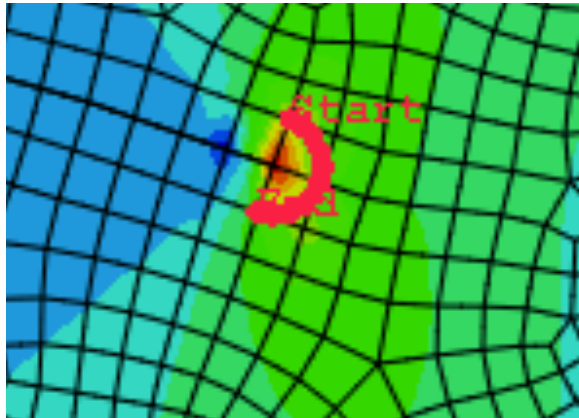


Fig 32 Integral path illustration at crack tip

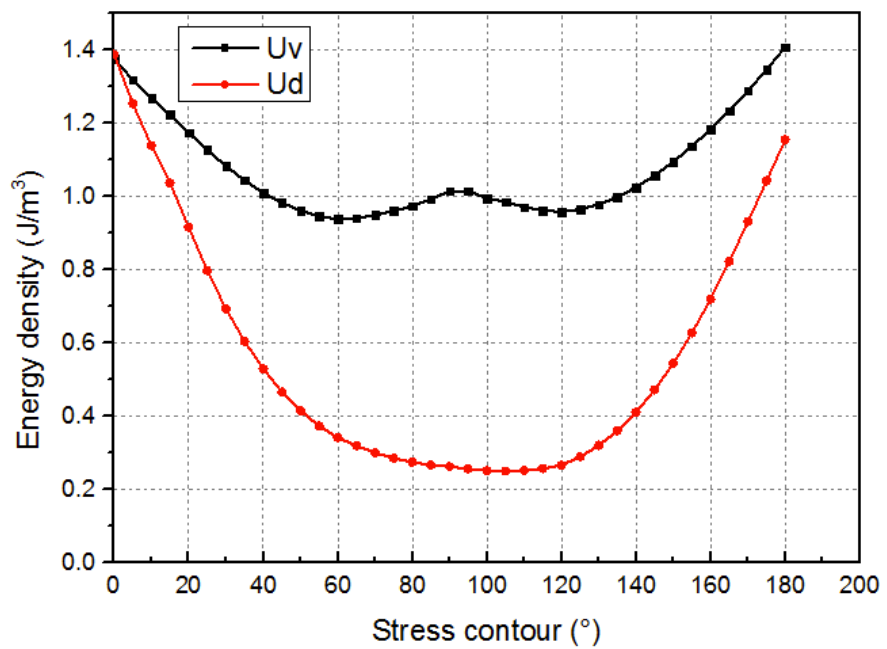


Fig 33 Distribution of Distortion energy density and Dilatational energy density at extended crack tip

## 4.5 Summary

In this section, the crack extension within resin layer was examined by fracture criterion based on SERR. The following results has been found that:

(a) After crack kinking into resin layer, the extension is dominated by geometric properties and even though crack path has fluctuation, it will propagation at kinked direction.

(b) The present of circular void can curve the crack extension direction. The curving effect becomes effective when voids are placed within 0.2mm from crack front.

(c) Crack extension in resin is a brittle fracture process that critical brittle failure condition is satisfied.

## 5. CONCLUSIONS

The main object of this research is to quantitatively investigate the influence of size, shape and distribution of manufacturing induced voids on delamination crack kinking.

The problem has been simplified as a DCB specimen with tensile loading at two arms. In the numerical exploration, a 2D FE model has been simulated and various conditions of voids were considered. A Mixed-mode fracture criterion was applied to evaluation delamination crack extension. The simulation helps to clarify the effects of voids on Mode I dominated crack kinking and extension. As discussed in[22], the stress oscillation caused by voids has a 0.5 mm range of influence. Voids have contribution on crack curving as long as the distance between void and crack tip is small. In composites, the delamination crack jumping will break the integrity of neighboring ply. Voids which causing delamination kinking may in the same time delay the breakage of next interface by curving the kinked resin crack. The actual composite in-service condition should be more complex and more combination of mode mixity can be considered in future work.

## REFERENCES

- (1) Mandell, J.F., D.D. Samborsky, And D. Cairns, Fatigue of Composite Materials and Substructures for Wind Turbine Blades, in Other Information: PBD: 1 Mar 2002. 2002. p. Medium: ED; Size: 279 pages.
- (2) Fuchs, E.R.H., et al., Strategic materials selection in the automobile body: Economic opportunities for polymer composite design. Composites Science and Technology, 2008. 68(9): p. 1989-2002.
- (3) Jamison Rd, S.K., Reifsnider Kl, Stinchcomb Ww, Characterization And Analysis Of Damage Mechanisms In Tension–Tension Fatigue Of Graphite/Epoxy Laminates. Effects of Defects in Composite Materials, ASTM, 1984. Stp 836: p. 21–55.
- (4) Lambert, J., et al., 3D damage characterisation and the role of voids in the fatigue of wind turbine blade materials. Composites Science and Technology, 2012. 72(2): p. 337-343.
- (5) Narayan, S.H. and J.L. Beuth, Designation of Mode Mix in Orthotropic Composite Delamination Problems. International Journal of Fracture, 1998. 90(4): p. 383-400.
- (6) Shokrieh, M.M. and A. Zeinedini, A Novel Method for Calculation of Strain Energy Release Rate of Asymmetric Double Cantilever Laminated Composite Beams. Applied Composite Materials, 2014. 21(3): p. 399-415.
- (7) Schon, J., et al., A numerical and experimental investigation of delamination behaviour in the DCB specimen. Composites Science and Technology, 2000. 60(2): p. 173-184.
- (8) Robinson, P. and D.Q. Song, A Modified Dcb Specimen For Mode-I Testing Of Multidirectional Laminates. Journal of Composite Materials, 1992. 26(11): p. 1554-1577.
- (9) Chai, H., The characterization of Mode I delamination failure in non-woven,

- multidirectional laminates. *Composites*, 1984. 15(4): p. 277-290.
- (10) Bowles, K.J. and S. Frimpong, Void Effects On The Interlaminar Shear-Strength Of Unidirectional Graphite-Fiber-Reinforced Composites. *Journal of Composite Materials*, 1992. 26(10): p. 1487-1509.
  - (11) Chambers, A.R., et al., The effect of voids on the flexural fatigue performance of unidirectional carbon fibre composites developed for wind turbine applications. *International Journal of Fatigue*, 2006. 28(10): p. 1389-1398.
  - (12) Huang, H. and R. Talreja, Effects of void geometry on elastic properties of unidirectional fiber reinforced composites. *Composites Science and Technology*, 2005. 65(13): p. 1964-1981.
  - (13) Zhu, H., et al., Influence of Voids on the Tensile Performance of Carbon/epoxy Fabric Laminates. *Journal of Materials Science & Technology*, 2011. 27(1): p. 69-73.
  - (14) C.A. Howe, R.J.P., A.A. Goodwin, A Comparison Between Voids in RTM and Prepreg Carbon/epoxy Laminates. Book: Eleventh International Conference on Composite Materials, 1997. IV: Composites Processing And Microstructure: p. 46-54.
  - (15) Bush, M.B., The Interaction between a Crack and a Particle Cluster. *International Journal of Fracture*, 1997. 88(3): p. 215-232.
  - (16) Reis, P.N.B., et al., Effect of Interlayer Delamination on Mechanical Behavior of Carbon/Epoxy Laminates. *Journal of Composite Materials*, 2009. 43(22): p. 2609-2621.
  - (17) Jakobsen, J., J.H. Andreasen, and E. Bozhevolnaya, Crack kinking of a delamination at an inclined core junction interface in a sandwich beam. *Engineering Fracture Mechanics*, 2008. 75(16): p. 4759-4773.
  - (18) ABAQUS V6.12 Theory Manual, SIMULIA Worldwide Headquarters, Rising Sun Mills, 166 Valley Street, Providence, RI 02909–2499.
  - (19) Anderson, P.M., Small Scale Contact Conditions for the Linear-Elastic Interface Crack. *Journal of Applied Mechanics*, 1988. 55(4): p. 814-817.

- (20) He, M.-Y. and J.W. Hutchinson, Kinking of a Crack Out of an Interface. *Journal of Applied Mechanics*, 1989. 56(2): p. 270-278.
- (21) Valvo, P., A revised virtual crack closure technique for physically consistent fracture mode partitioning. *International Journal of Fracture*, 2012. 173(1): p. 1-20.
- (22) Krueger, R., Virtual crack closure technique: History, approach, and applications. *Applied Mechanics Reviews*, 2004. 57(2): p. 109-143.
- (23) W. S. Johnson, P.D.M., Influence of the Resin on Interlaminar Mixed-Mode Fracture. *NASA Technical Memorandum*, 1985.
- (24) Álvarez, V., et al., The influence of matrix chemical structure on the mode I and II interlaminar fracture toughness of glass-fiber/epoxy composites. *Polymer Composites*, 2003. 24(1): p. 140-148.
- (25) Ricotta, M., M. Quaresimin, and R. Talreja, Mode I Strain Energy Release Rate in composite laminates in the presence of voids. *Composites Science and Technology*, 2008. 68(13): p. 2616-2623.